

pubs.acs.org/JACS Perspective

Terahertz Circular Dichroism Spectroscopy of Molecular Assemblies and Nanostructures

Won Jin Choi, Sang Hyun Lee, Bum Chul Park, and Nicholas A. Kotov*



Cite This: J. Am. Chem. Soc. 2022, 144, 22789-22804



ACCESS I

Metrics & More

Article Recommendations

ABSTRACT: Chemical, physical, biological and materials engineering disciplines use a variety of chiroptical spectroscopies to probe geometrical and optical asymmetry in molecules and particles. Electronic (ECD) and vibrational (VCD) circular dichroism are the most common of these techniques and collectively enable the studies of electronic and vibronic transitions with energies between 0.1 and 5.0 eV. The vibrational states with characteristic energies in the range of 0.001-0.01 eV carry valuable information about concerted intermolecular motions in molecules and crystals involving multiple atoms. These vibronic transitions located in the terahertz (THz) part of the spectrum become increasingly more important for the chemistry, physics, and biology of complex molecules and materials However, the methodology and hardware of THz circular dichroism (TCD) are much less developed than the chiroptical spectroscopies for ultraviolet, visible, near- and mid infrared photons. Here we provide theoretical foundations, practical implementations, comparative assessments, and exemplary applications of TCD spectroscopy. We show that the sign, intensity, and position of TCD peaks are highly sensitive to the three-dimensional structure and long-range organization of molecular crystals, which offer unique capabilities to study (bio) molecules, their crystals, and nanoscale assemblies and apply the novel data processing methodologies. TCD also offers a convenient toolbox to identify new physical phenomena, such as chiral phonons and their propagation in nanostructured matter. We also discuss the major challenges, emerging opportunities and promising research directions, including broad investigation of chiral phonons observed in chiral (nano) crystals and emerging machine learning methodologies for TCD in biological and nanoscale structures. Ubiquity of low-frequency vibrations with rotational components in biomolecular structures, combined with sharpness of peaks in TCD spectra, enables a variety of technological translations.

■ INTRODUCTION

Different forms of chiroptical spectroscopy are needed for experimental and theoretical studies of a variety of chiral objects, molecules, and materials at numerous scales in chemistry, physics, biology, pharmacology, and nanotechnology.^{1,2} The high information content and ubiquity of chiral compounds also make these spectroscopies valuable for application of data science for biological analysis and materials discovery. Within the realm of chiroptical spectroscopies, electronic circular dichroism (ECD) and vibrational circular dichroism (VCD) have been used the most frequently³⁻⁵ and have enabled the identification and quantification of mirror asymmetry at molecular, nanometer, and micrometer scales. ECD characterizes electronic transitions between the ground and excited quantum states of molecules (1.5-5 eV), while VCD provides information about vibrational states in the ground electronic state of molecules (0.1–0.5 eV) (Figure 1). Other chiroptical spectroscopies are used less often but still offer valuable information about the chemical and physical properties of gases, liquids, and solids. They include, for instance, circularly polarized luminescence (CPL) spectroscopy that measures the differential emission intensity between right- and left-circularly polarized (RCP and LCP, respectively) photons being excited with a nonpolarized light source. Most often CPL is associated with the chiral ground or excited states of molecules and, therefore, covers approximately the same range of energies as ECD. The signal-to-noise ratio

(SNR) of CPL is, however, at least 10 times lower than that of ECD because of low values of anisotropy factor, g_{lum} , for molecules—typically in the range of $\sim 10^{-3}$ to $10^{-4.6}$ The values of g_{lum} increase, however, when chiral emitters are attached to inorganic nanoparticles (NPs) due to chiroptical effects specific for nanoscale inorganic matterials.^{7,8}

Raman optical activity (ROA) measures the difference between inelastically scattered RCP and LCP light. ROA spectroscopy covers the energy range between 0.02 and 0.2 eV and provides data on vibronic states of molecules and nanostructures complementary to VCD^{10,11} because many VCD vibrational modes are forbidden, but are allowed for ROA. A big advantage of ROA compared to other methods of chiroptical spectroscopy is that it may be used to evaluate samples of dispersions in water that can be too absorptive for VCD. 12

In recent years, several nonlinear chiroptical methods have also emerged, such as hyper-Rayleigh scattering (HRS), chiral sum frequency generation, and third harmonic Mie scattering

Published: December 9, 2022





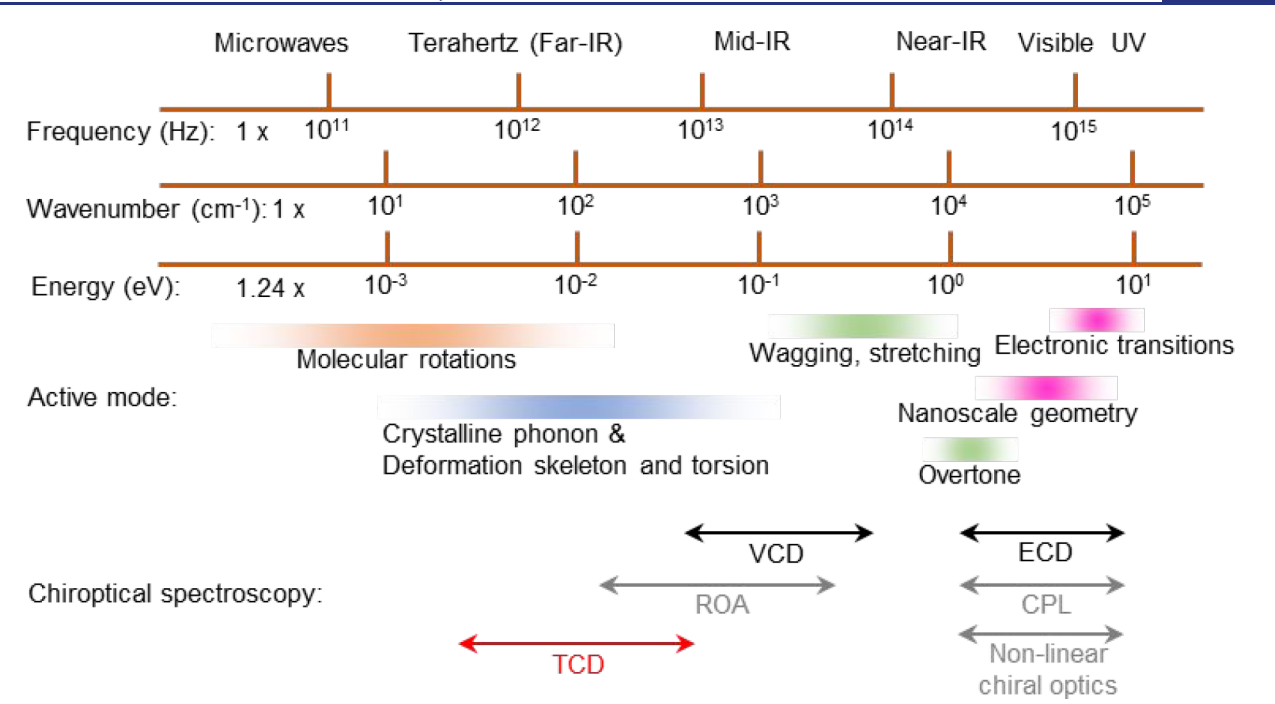


Figure 1. Different spectroscopic modalities, vibrational modes, and characteristic excitation energies of chiroptical spectroscopies. ECD spectroscopy is often referred to as CD spectroscopy. Such notations are typical for many fields of research including chiral organic, inorganic, and biological nanostructures, but in the context of this article we suggest using ECD terminology to better differentiate the vibrational states characterized by different spectroscopic modalities.

(THMS). 13-15 These methods are being developed to address a major drawback of linear chiroptical methods, that is, the small absolute difference between signal amplitudes for left and right enantiomers. 16 For instance, the traditional scales for ECD spectra are in millidegrees of ellipticity, signifying that the difference in absorption of RCP and LCP by chiral molecules amounts to only fractions of a percent, hence the high noise and low spectroscopic sensitivity. The difference in signal amplitudes for nonlinear chiroptical methods is much larger. 16 Five orders of magnitude enhancement of optical activity was observed for HRS of Ag plasmonic nanohelices. 14 In addition to plasmonic nanostructures, several chiral π -conjugated polymers with high hyperpolarizabilities, such as helicenes, have also shown markedly enhanced HRS response due to their intrinsic electronic delocalization. 17,18 The range of ellipticities observed for THMS is a thousand times greater than for ECD; ellipticity as high as three degrees was achieved for CdTe nanohelices. 15 Another advantage of the nonlinear version of chiroptical spectroscopies is that they do not require a large volume of sample. For example, the typical interaction volume for HRS that was regarded as small was in the range of 10-100 pL¹⁶ and, for THMS, it experimentally determined for volumes as small as $\ll 1 \mu L$. However, nonlinear chiroptical spectroscopies also have weaknesses: (i) the overall signals are weak because of intrinsically inefficient light-matter interactions for higher-order nonlinearities and (ii) experimental realizations of these methods are complex, often requiring multiple femtosecond lasers. 14,15,19-23

In contrast, the optical signals of nanometer scale structures can be substantially enhanced, suggesting possible solutions for the problems of linear and nonlinear chiroptical spectroscopies. Local field enhancement in plasmonic assemblies^{24,25} could provide otherwise inaccessible spectra with the information on dynamics of inorganic and biological

nanostructures. 14,19,20,22,23,26 For example, ROA spectra are approximately 10³ times lower in intensity than typical Raman spectra, 9 but can be enhanced using nanoscale plasmonic particles. 10,11,27,28 In addition, chiral nanomaterials, such as plasmonic nanohelices, enhance optical nonlinearity from higher-order multipoles including magnetic dipoles. 14 Analogous to conductive magnetic coils that can drive current along the longitudinal direction, chiral nanostructures can induce a magnetic field parallel to the induced electric dipole, leading to enhanced optical chirality. Tightening of density of states at nanoscale as well as strong chiroptical signal from circular-polarization-selective scattering off chiral structures are beneficial for the field enhancement, too. 29

Chiroptical spectroscopies for energy states in the range of 0.001-0.01 eV, including terahertz circular dichroism (TCD) are much less developed than all other spectroscopy techniques albeit they carry a lot of information about different types of collective vibrational modes (Figure 1). The chiroptical techniques described above have difficulties accessing the vibronic states involving large molecular weight segments or concerted motions of a large number of atoms. At the same time, chiroptical spectroscopies for low-energy photons are much needed because of the commonality of such vibrational states in biomolecules, crystals, nanoassemblies, nanobio superstructures, two-dimensional (2D) materials, and many other complex structures and have been attracting a lot of attention recently. The spectroscopy suitable for the energy range of these vibronic and phononic modes is terahertz (THz) time domain spectroscopy (THz-TDS). However, the typical implementation of THz-TDS does not allow resolution of dichroic effects related to circular polarization of absorbed or emitted THz photons. THz-TDS has the capability to characterize low-frequency vibrational states of complex molecules and nanomaterials 30,31 that can be

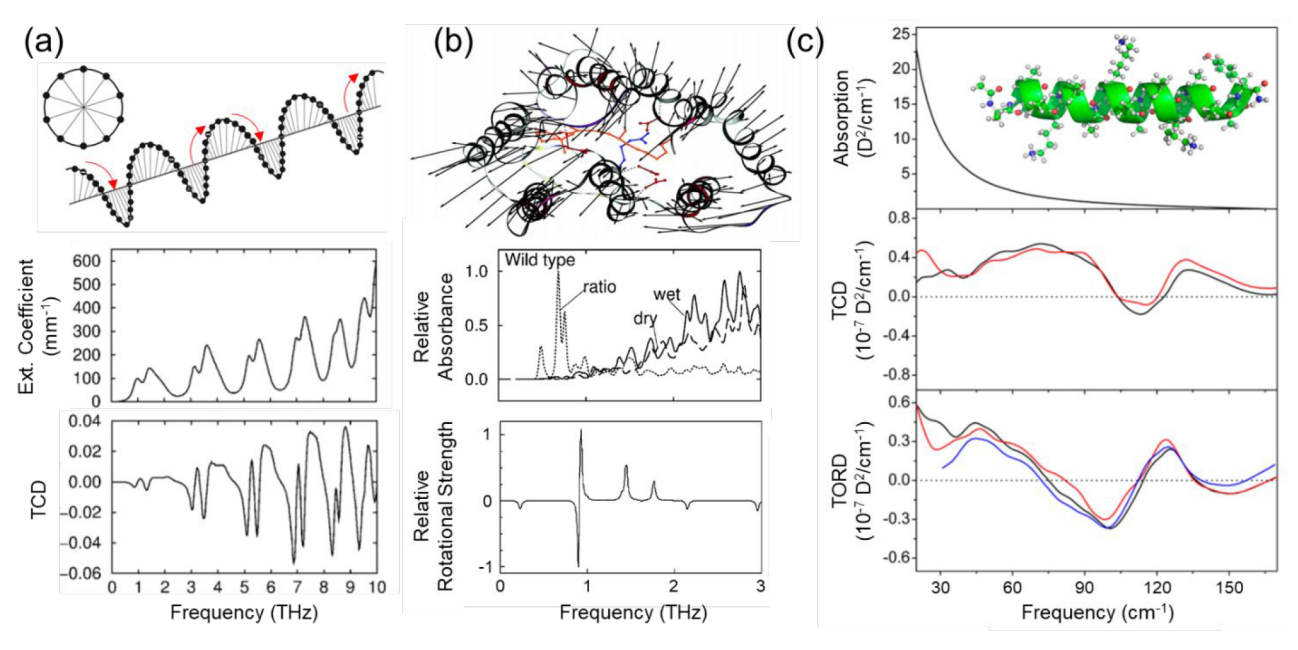


Figure 2. (a) Theoretical helical model of a macromolecule and its extinction coefficient and TCD spectra. (b) Structure of bacteriorhodopsin with corresponding absorbance and rotational strength spectra, which is closely related to the TCD in the THz range. Arrows in the schematic of bacteriorhodopsin indicate the low-frequency mode atomic motions at 0.498 THz. Reprinted with permission from ref 56. Copyright 2003 Mary Ann Liebert, Inc. (c) MD simulation of TA, TCD, and THz optical rotatory dispersion (TORD) spectra of the α-helical polypeptide. TCD and TORD spectra obtained from cross-correlation functions $\langle \mu(t)\cdot M(0)\rangle$ (black line) and $\langle \mu(0)\cdot M(t)\rangle$ (red line). The TORD spectrum (blue line) obtained by carrying out the Kramers–Kronig (K–K) transformation of the TCD spectrum. Reprinted with permission from ref 57. Copyright 2014 American Chemicay Society.

extended to the nanoscale assemblies thereof in the form of composites⁵ or other hybrid materials. ^{32,33} THz spectra can also provide valuable information about fine details of molecular structure and packing conformation of crystals from small molecules representing metabolites, ^{34,35} pharmaceuticals, ^{36,37} and explosives. ³⁸ Macromolecules with nanoscale dimensions such as deoxyribonucleic acid (DNA) and proteins also show structure-specific THz signatures. ^{31,39,40} For instance, THz absorption can be sensitive to the sequence of nucleic acids and hybridization of DNA, ^{41,42} where single-base mutations lead to changes in peak position. ⁴³ However, for nearly all of applications, broad difficult-to-resolve THz absorption peaks are typically observed, making it difficult to confidently identify specific vibrations in complex molecular structures based solely on intensity versus frequency data.

Comparison with other spectroscopic modalities also brings up the question about selection rules for THz spectra and TCD-active modes similarly to IR- and Raman-active modes. As a brief reminder, vibrational modes are IR-active when such mode is associated with the large changes in the dipole moment, whereas vibrational modes become Raman-active when they are associated with large changes in polarizability. Although the TCD selection rules might be expected to be similar to those for IR active modes, they are more "permissive" than those for chiroptical spectroscopies because the vibrations associated with THz frequencies typically involve large number of atoms and, thus, are associated both with the some change of dipole and polarizability. Some THz bands are also superpositions of multiple vibrational states that are close in energy but with different symmetries. For THz vibrations associated with the long-range order exemplified by chiral phonons (see below), the requirement of translation invariance restricts the spectrum to predominantly IR active modes.4,44

In-depth understanding of the origin of the spectral resonances and resolving overlapping peaks require a chiroptical spectroscopy conceptually similar to ECD and VCD that can be termed THz circular dichroism (TCD). Since LCP and RCP make absorption differences sensitively depend on the chirality of 3D molecular organization, ⁴⁵ TCD is better suited for resolving complex molecular motions responsible for these vibrations than normal THz-TDS. For example, TCD is essential for characterization of protein conformation, their intermolecular interactions with ligands, 46,47 dynamics of lipid membranes, and shells of water around various nanoscale structures. 40 Also important, the concerted motion of highmolecular weight segments leads to chiral normal modes due to frequent chirality of constituents, the asymmetry of multiatomic geometries, and rotational components of these vibrations. One of the special cases is represented by chiral phonons. These vibrations are collective mirror-symmetric movements of atomic groups connected by primary and secondary chemical bonds. Some chiral phonons for special cases of two-dimensional materials have been detected in the IR part of the spectrum, 50,51 but numerous chemical structures, exemplified by biological crystals and nanoscale assemblies, are expected to display chiral phonons in the THz range for which TCD will be essential.

TCD spectroscopy offers the ability to uncover optical phenomena that were hitherto "invisible" to other chiroptical techniques. For example, ECD can identify excitations in the UV to visible range related to twisted aromatic states with $\pi\pi^*$ transitions. TCD elucidates of the spectrum, exemplified by interatomic vibrations of covalent bonds such as amide I vibration and amide II vibration. While these methodologies unveil atomic scale phenomena, TCD elucidates chirality of the long- and short-range

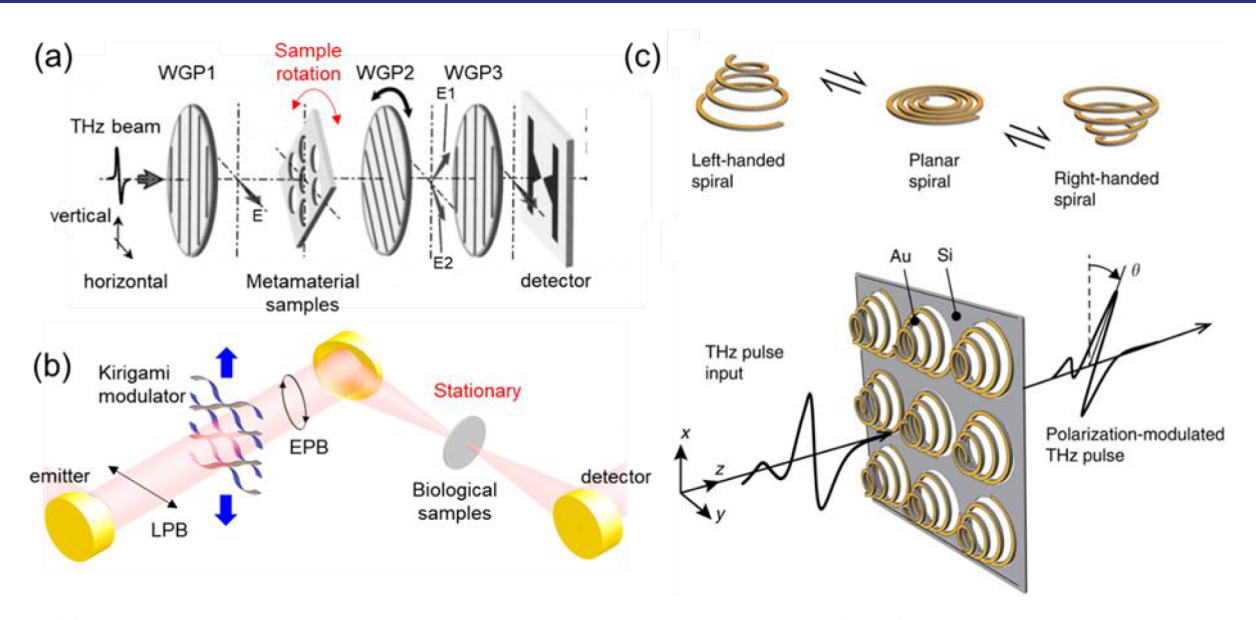


Figure 3. (a) Schematics of THz time-domain polarimetry using three wire grid polarizers (WGP). Reprinted with permission from ref 62. Copyright 2013 AIP publishing. (b) Practical TCD spectroscopy with kirigami polarization modulator; LPB and EPB indicate the linearly and elliptically polarized beams, respectively. Reprinted with permission from ref 5. Copyright 2019 Springer Nature. (c) Chirality-switchable metamaterial, which can be achieved by changing the deformation direction of an Archimedean spiral. Reprinted with permission from ref 65. Copyright 2015 Springer Nature (CC-BY 4.0).

intermolecular vibrations. TCD spectroscopy can also shed light on the identity and anharmonicity of many coupled modes in large assemblies connected by supramolecular bonds, because TCD enables one to mitigate severe broadening of typical THz absorption spectra "lumping" multiple transitions into one broad featureless band. This is especially typical for many biomolecular complexes. For example, there were no apparent absorption sharp peaks observed in the THz absorption spectra for insulin fibrils, ⁵⁴ myelin basic proteins, and lipids. ⁵⁵

To understand better the prospects and capabilities of TCD in the studies of a diverse array of chiral materials, biological structures, and physical phenomena, we review herein the theoretical and experimental developments in TCD followed by a discussion of the major challenges and opportunities for measurements of THz chiral vibrational modes.

■ THEORETICAL FOUNDATIONS OF TERAHERTZ CIRCULAR DICHROISM IN BIOMOLECULES

While TCD can be observed for a variety of chemical structures, biomolecules offer a comprehensive model for understanding the origin and significance of low-energy vibronic states in the THz range. THz optical activity of biomolecular complexes was initially predicted by normalmode analysis using a simple mass and spring model of a spiral, which served as a simplified representation of a macromolecule with similar geometry (e.g., α -helix, twisted ribbon, spiral).⁵⁶ Several low-frequency modes below 3 THz were concerted motions of the molecular spirals (Figure 2a) corresponding to acoustic phonons with torsional components. These modes generate a large change in dipole moments rendering them optically active. Additional studies showed that mechanical models of protein molecules, for instance, bacteriorhodopsin (Figure 2b), also exhibited chiral vibrations involving out-ofplane distortions such as twists and in-plane helix translocations in the THz range.⁵⁶

The existence of the chiral normal modes was confirmed by atomistic simulations using density function theory (DFT) and molecular dynamics (MD) (Figure 2c). MD trajectories of α helical polypeptides suggest that the angular component and magnetic dipole moment of helical polypeptides are sufficiently intense to be experimentally detected by TCD spectroscopy. A noteworthy prediction made by this study was that TCD and THz optical rotation dispersion (TORD) spectra should display distinct positive and negative peaks at 2.24, 3.44, and 4.04 THz (Figure 2c, middle and bottom) as opposed to the THz absorption spectrum of an α -helical polypeptide with featureless, monotonically decreasing peaks (Figure 2c, top). This theoretical prediction that can be extended to a variety of biomolecules underscores the potential of TCD and TORD as a powerful toolbox to obtain data about the conformation and dynamics of large molecules as well as nanoscale structures with chiral geometries.

METHODOLOGY OF TCD FOR TIME-DOMAIN SPECTROSCOPY

The technical setup for TCD is fundamentally different from that for ECD or VCD. The light sources in ECD and VCD are continuous, and the diffraction gratings or interferometerbased optical setup, such as Michelson systems, are used to obtain spectral data. The typical choices of detectors are photomultiplier tubes or amplified photodiodes. For example, Fourier Transform VCD (FT-VCD) spectroscopy utilizes a Michelson interferometer and diffraction grating, measuring Fourier transformable signals by applying different weights based on the mirror position.⁵⁸ In contrast, THz spectroscopy uses short pulses of THz radiation in time-domain configuration. Widely used methods for generation and detection of THz pulses include photoconductive antennae (PCA) and crystals, such as ZnTe, GaP, and GaSe with femtosecond lasers. With applied voltage across PCA, nonlinear optical rectification takes place in the femtosecond laser pulse, generating THz pulses. These PCA and crystals for

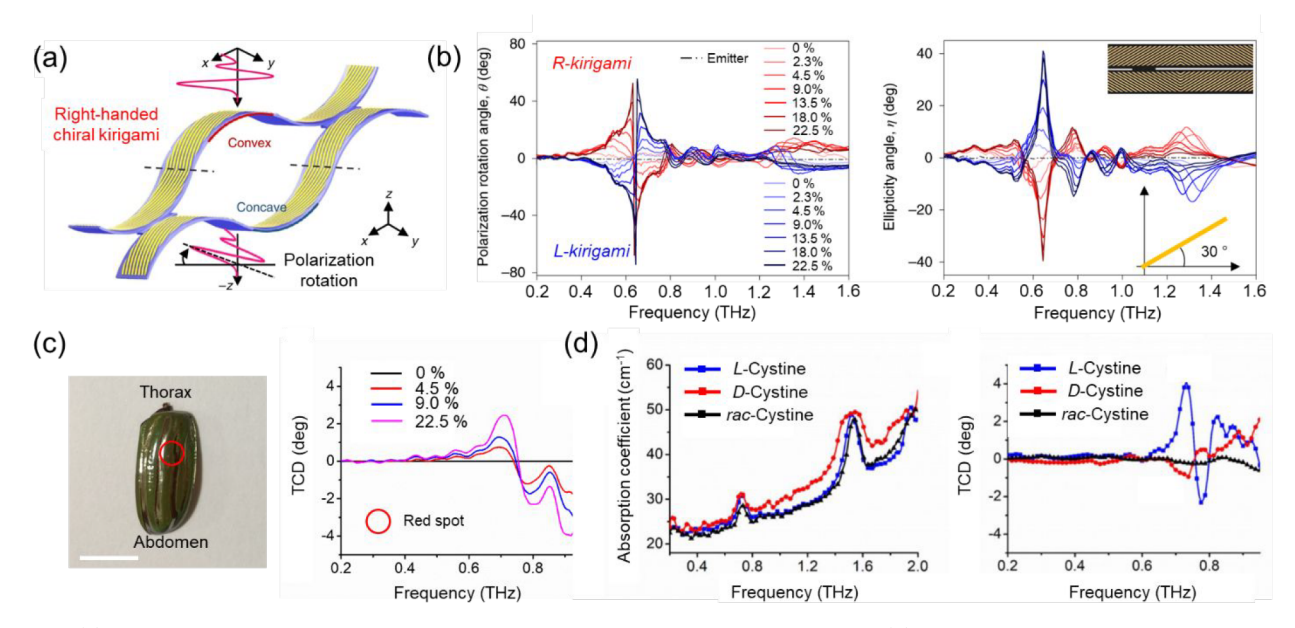


Figure 4. (a) Schematic of chiral plasmonic kirigami sheets as a circular polarization modulator. (b) Polarization rotation angle and ellipticity of kirigami metasurfaces with slanted Au strips (angles of 30°) for different strain (0–22.5%). Inset shows optical microscope image of kirigami sheet before stretching. (c) Image of an elytron of C. gloriosa and corresponding TCD spectra measured by a kirigami modulator without sample rotation. Four different values of strain (%) of kirigami modulators are measured, and the red circle indicates the location of measurement. Scale bar, 1 cm. (d) THz absorption coefficient and TCD results of L-, D-, and *rac*-cystine. Reprinted with permission from ref 5. Copyright 2019 Springer Nature.

THz-TDS are dependent on the photon energy and also the polarization of the electromagnetic field as their detecting and generating mechanisms are based on metal dipole antenna pattern and linear birefringence of optical rectification, respectively. Also, by scanning the delay line, the electric field (E) amplitude and phase of the THz waveform can be registered as a function of time. For this reason, THz-TDS can directly measure the transient electric field (E) in the time-domain format making possible the calculation of ellipticity once the electric fields in the horizontal, E_{xy} and vertical, E_{yy} directions, are obtained. Details of the experimental set-ups are beyond the scope of this paper and can be found in corresponding references.

The practical implementation of ECD and VCD is based on variable circular polarization of light by piezoelectric modulators at quarter-waveplates. However, while this polarization modulator is common for visible and NIR parts of the spectrum, they are uncommon for THz light. Typically, photoelastic materials, such as fused silica and calcite (for UV to visible range) and MgF2 and ZnSe (for near- to mid-IR), are used for quarter waveplate modulators, converting linearly polarized light into CPL for ECD and VCD. However, effective quarter waveplate modulators for the THz range of beam do not yet exist and still need to be developed. Thus, the development of TCD requires a different technical setup with appropriate optical elements and methodologies.

Experimental methods for the characterization of chiroptical properties in the THz range have been devised initially for metamaterials, which could be readily verified by electromagnetic simulations. Si,62-65 Miyamaru et al. demonstrated THz-TDS-based polarimetry using three linear polarizers (WGP1, WGP2, WGP3) to measure polarization changes of THz waves through the two-dimensional photonic crystals by tilting the incident angles (Figure 3a). By rotating the polarization axis of WGP2, one can detect E_x and E_y after

passing through the sample. WGP1 and WGP3 are used for accurate detection of the electric fields corresponding to the antenna orientations of the emitter and detector, respectively. The TCD measurements using the method shown in Figure 3a require, however, intermittent rotation of the sample relative to the incident linearly polarized light to remove the contribution of linear birefringence.

The most common protocol for obtaining TCD spectra involves acquisition of THz spectra in transmission mode, carried out twice at different sample rotation angles.⁶⁵ Between the first and second measurements, the sample is rotated by 90° around the light propagation axis. Reliable TCD spectra of micromanufactured metamaterials can be obtained using this method because the periodicity of their structures or sample homogeneity is high-approximately an order of magnitude longer than the wavelength of the beam. However, the sample rotation method is not convenient or feasible for the majority of biomaterials especially when the size of the sample is microto nanoscale because small inaccuracies of spot position caused by rotation leads to very large artifacts.⁶⁶ To solve this problem, TCD spectroscopy with polarization modulators is needed to make observation from the stationary sample possible (Figure 3b). Ideally, enantiomerically switchable modulators (Figure 3c) with broad-band optical activity and high-frequency modulating capability are preferable as polarization modulators for TCD spectroscopy.

TCD spectroscopy is associated with additional difficulties that need to be taken into account when studying molecular assemblies and nanostructures. (1) Due to long lengths of photons (\sim 300 μ m) in the THz region, the size of the focused beam spot is larger (approximately hundreds of micrometers) than those used in the UV, visible, and IR range, which means that large amounts of sample are needed to accomplish reasonable photon–phonon interactions. (2) The large absorption coefficient of water in the THz range may often

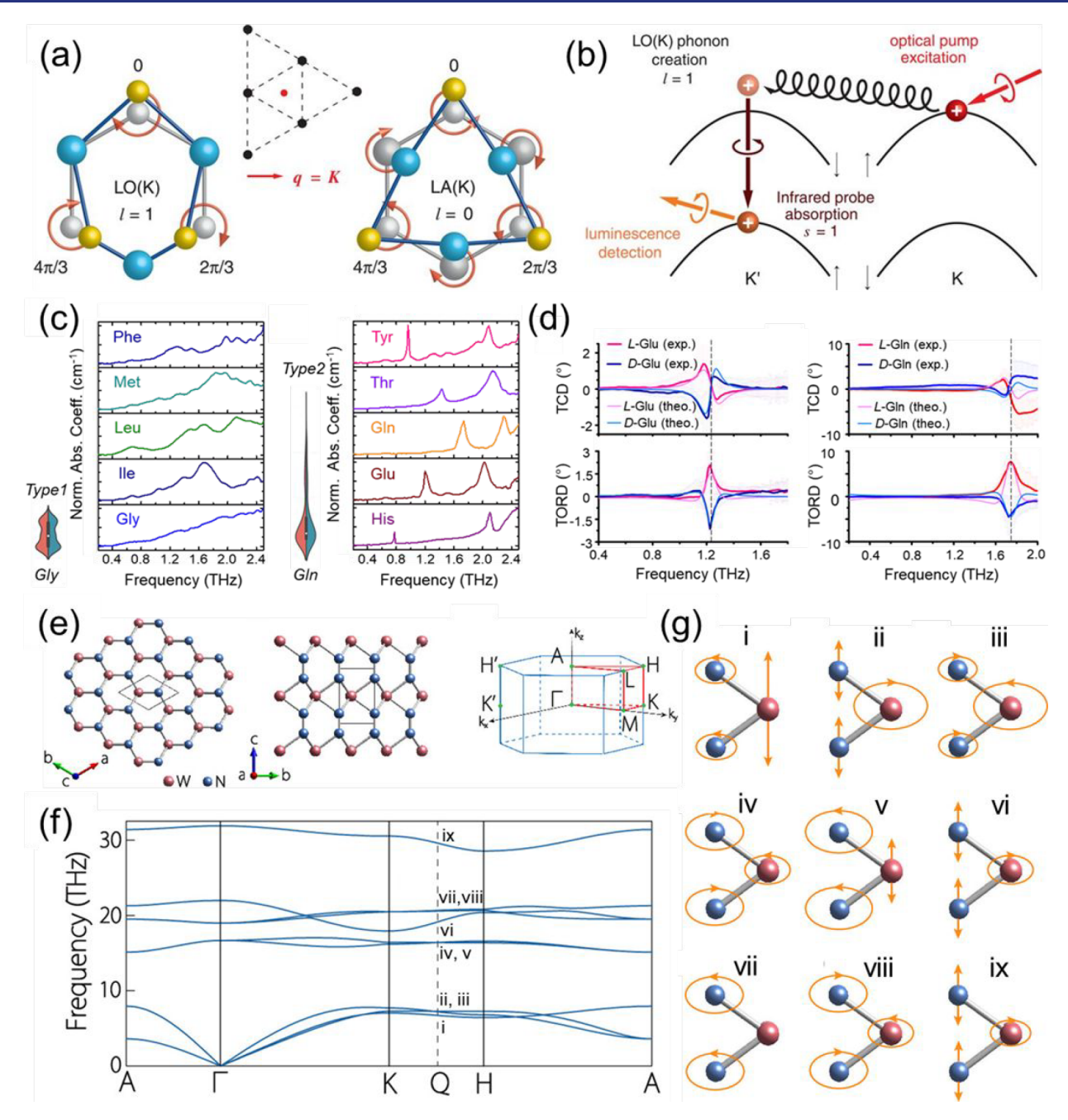


Figure 5. (a) The atomic motion of W and Se atoms in real space is intrinsically chiral at the K point (red dot) due to the threefold rotational symmetry. (b) Process for the intervalley optical transition of holes explaining angular momentum conservation. Reprinted with permission from ref 50. Copyright 2018 The American Association for the Advancement of Science. (c) Normalized THz absorption (TA) spectra of five representative L- amino acids with broad peaks and sharp peaks, respectively. Broad peak AAs — Type 1, space group = $P2_1$ or C2; sharp peak AAs — Type 2, space group = $P2_12_12_1$. (d) Experimental and calculated TCD and TORD spectra of Glu and Gln, respectively. Reprinted with permission from ref 48. Copyright 2022 Springer Nature. (e) Top and side view of WN₂ crystal and BZ of WN₂. The black box indicates the unit cell. (f) Brillouin zone of WN₂. Note that Q is the midpoint of the K—H path. (g) Vibration patterns of phonon modes at point Q. Reprinted with permission from ref 79. Copyright 2021 American Chemical Society.

lead to a high noise level. Currently, TCD signals with time-domain spectroscopy above 0.5 deg are considered as an acceptable level, which is still much higher than other chiroptical methods with typical signals of only a few mdeg. At the higher frequency range (>2 THz), the signal-to-noise (S/N) level is extremely low due to the low power of the modern THz emitter. The development of high-power THz emitters will mitigate this problem.

TCD Spectroscopy with Modulated Quarter Waveplates based on Kirigami Nanocomposite Sheets. Development of practical TCD spectroscopy has been hindered by the difficulties with polarization modulation of THz radiation. 5,65,66 A few examples of static quarter waveplate-like materials and devices were developed, but dynamic polarization modulation in real-time and realization of TCD spectroscopy has not been accessible. 65,67–69 Recently, a method for the practical TCD spectroscopy of biomaterials

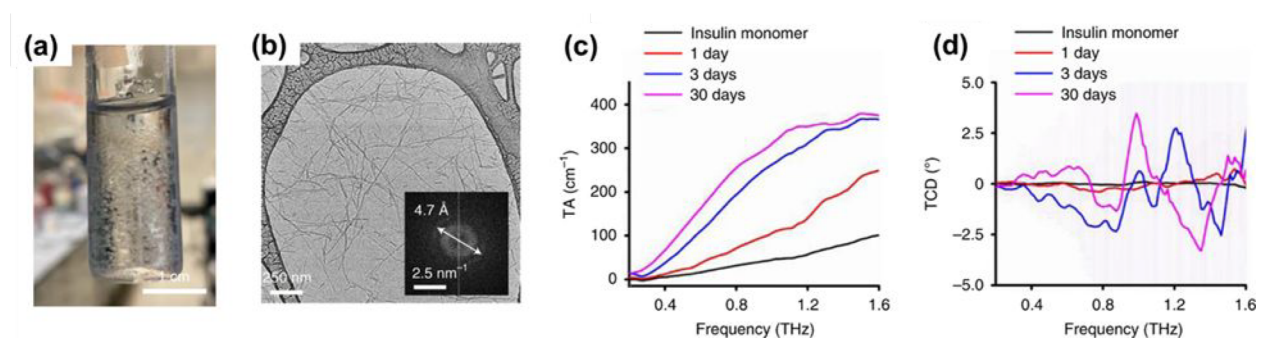


Figure 6. (a) Photograph of insoluble insulin fibrils formed at pH 2. Scale bar is 1 cm. (b) TEM image and selected-area electron diffraction pattern of insulin fibrils. TA (c) and TCD (d) spectra of insulin from monomers to 30 days of fibrillation. The data in (c) and (d) are presented as mean values \pm s.d. Reprinted with permission from ref 48. Copyright 2022 Springer Nature.

was enabled by the chiral plasmonic sheet inspired by kirigami paper art (Figure 4a).⁵ Being a topologically equivalent helix structure, the kirigami metasurfaces modulate the polarization rotation and ellipticity angle of the THz beam up to 80° and 40°, respectively, under application of mechanical strain of 22.5% (Figure 4b).

TCD spectra of several biological samples including an elytron of the green beetle, a leaf of the sugar maple tree, a dandelion petal, and pellets of cystine dipeptides (L-, D-, and rac-cystine) were measured without sample rotation (Figure 4c,d). Among them, the chiral phonon mode was experimentally observed from the cystine crystals showing mirror-like TCD spectra between L- and D-cystine at a resonant frequency of approximately 0.73 THz (Figure 4d). Following this result, L-cystine's asymmetric absorbance of left- and right-circularly polarized THz beams was also revealed by McDonnell et al. Using chiral THz emitters based on Pancharatnam—Berry phase nonlinear metasurfaces.

■ TCD SPECTROSCOPY OF CHIRAL PHONONS IN NANOMATERIALS AND BIOMOLECULES

After the practical realization of TCD spectroscopy and its potential as a nondestructive modality for several biological samples was demonstrated, the TCD investigation of biological molecules and other chiral nanomaterials have been actively established. Among them, one notable result is the observation of chiral phonon modes in biomolecular complexes.

Chiral phonons in biomolecular crystals and nanofibrils are central to the comprehension of intermolecular interactions since TCD provides unique signatures of the conformation, phase, and hydration of biomolecular organizations. They are also strongly related to the dynamic mechanisms of many biological functions of macromolecules such as proteins and lipids. Analysis of TCD spectra leads to a better understanding of chirality of these molecular structures and nanomaterials by direct observation of chiral vibrational modes.

Chiral phonons have been studied hitherto in a very limited set of materials such as two-dimensional hexagonal lattices of MoS_2 and WSe_2 that display spectroscopic signatures in the near-IR part of the spectrum between 0.5 and 2 eV. 50,51,76,77 Zhang et al. 76 observed the chiral phonons at Brillouin zone (BZ) corners that are strongly coupled with circularly polarized IR photons taking advantage of a valley phonon Hall effect (Figure 5a,b).

The use of ROA enables registration of chiral phonon modes in nanoparticles from Co_3O_4 with the chiral distortions in the

crystal lattice. ⁷⁸ Observation of chiral phonons from a slurry of crystalline amino acids was also achieved by acquiring spatially resolved THz absorption (TA), TCD, and TORD spectra. ⁴⁸ Since phonons are strongly correlated to the symmetry of crystal structures, space group dependent phononic signatures were found. ⁴⁸ The associated sharp TCD and TORD peaks were also identified in microcrystals of several other amino acids (His, Gln, Glu, Thr, and Tyr) that crystallized in a $P2_12_12_1$ space group (Figure 5c,d). Theoretical studies of chiral phonons revealed that two-dimensional nanomaterials, such as WN₂, MoN, and MoP could sustain chiral phonon modes along the high-symmetry paths in the BZ (Figure 5e-g). ⁷⁹

Chiral phonon's strong sensitivity to the chemical interactions in the crystal lattice predicates their utility for biomedical industry and chiral photonic applications. TCD spectroscopy can be, for instance, utilized in in medicine quality control and biomedical imaging, 80,81 photonic devices that require electron—phonon coupling, and the phonon-driven topological states of solids. 50,82

■ FUTURE DIRECTIONS

Biomedical Applications of TCD. TCD can be particularly important in the pharmaceutical industries, where the quality of drugs should be continuously monitored in noncontact and nondestructive manners. TCD enables fast real-time inspection of drugs for the presence of unwanted enantiomers. The need for thorough online quality control over chiral drugs is well documented by the exceptionally harmful side effects of thalidomide, whose one enantiomer caused birth defects while the other one did not.

The efficacy of drugs can be affected by chemical (thermolytic, oxidative, or photolytic degradation), physical (polymorphic changes, hydration, and dehydration), or microbiological (failure of preservative) instability. TCD spectroscopy can be integrated in the manufacturing, processing, transporting, and storing of packaged drugs, which is difficult for ECD and VCD because packaging materials are opaque in the visible/IR spectral range but are transparent for THz photons. Both solids and liquids could be examined by this noncontact, nondestructive, and nonionizing method, and their TCD or spectral phononic signatures would be easily registered.

The significance of TCD for biomedical applications can also be highlighted by the observation of chiral phonons in the nanofibrils of amyloid peptides. Distinctive positive and negative TCD peaks showed higher spectral resolution than the broad TA spectra (Figure 6). Amyloid fibers from a variety

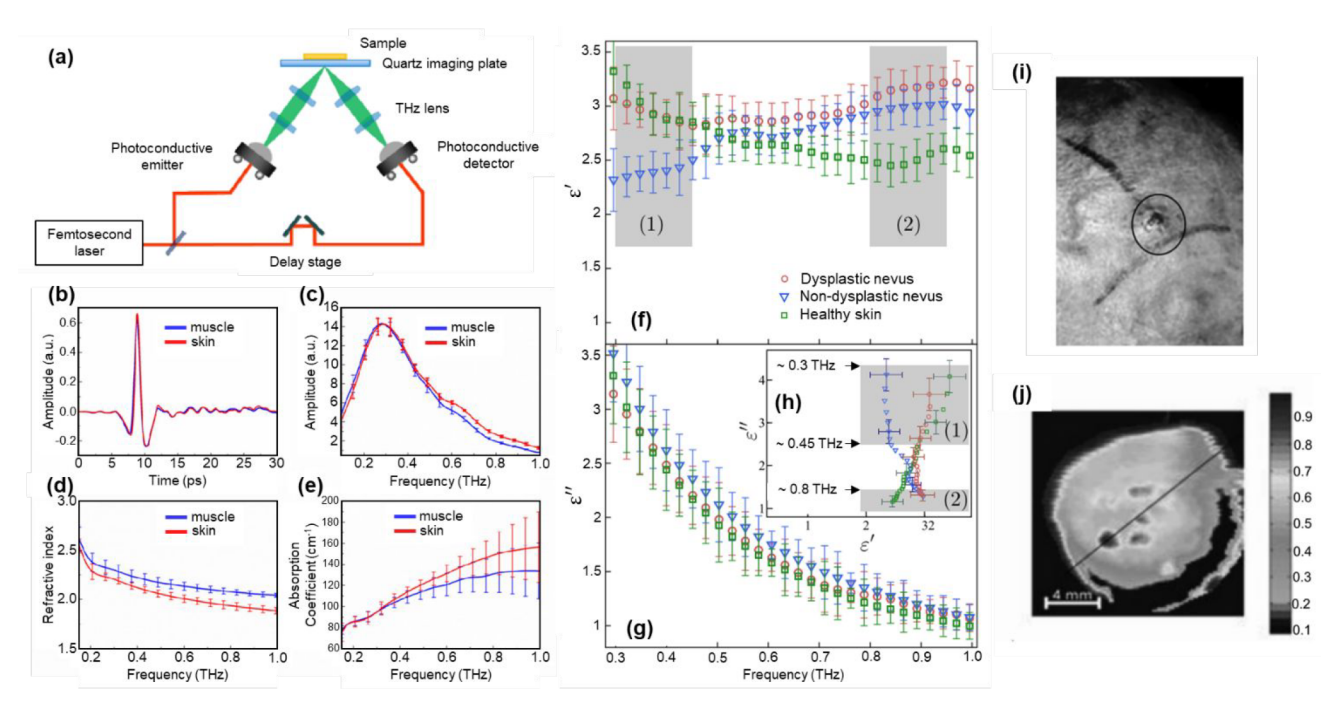


Figure 7. (a) Schematic diagram of the reflective THz spectroscopic and imaging system for biological samples. (b) Average time-domain THz signal of the fresh muscle and skin tissues (n = 6). (c) Corresponding average frequency-domain spectrum of (b). (d) Calculated refractive index, and (e) Absorption coefficient of the fresh muscle and skin tissues with the standard deviations (n = 6). Reprinted with permission from ref 92. Copyright 2017 The Optical Society. (f-h) THz dielectric characteristics of healthy skin (green), nondysplastic (blue), and dysplastic (red) nevi. Reprinted with permission from ref 93. Copyright 2015 AIP Publishing. (i) Photograph of a skin sample and (j) a THz image of a skin sample, in which the central dark regions with increased absorption correspond to the basal cell skin cancer. Reprinted with permission from ref 94. Copyright 2003 SPIE.

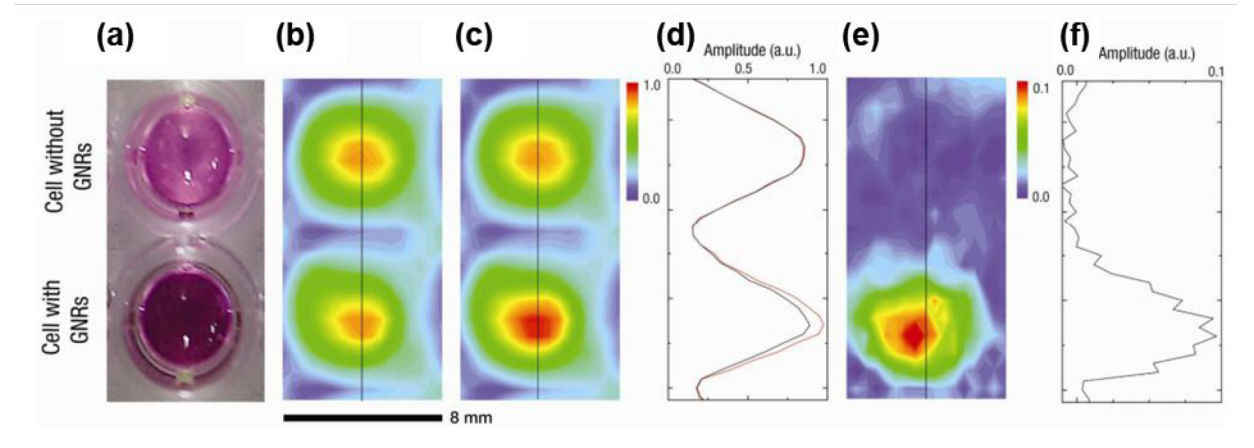


Figure 8. Cancer cell images with and without Au nanorods. (a) Visible image, (b) THz mapping without IR irradiation, (c) THz mapping with IR irradiation, (d) Amplitudes along the lines in (b, black) and (c, red), respectively. (e) Differential image between (b) and (c). (f) Signal amplitudes along the line in (e). Reprinted with permission from ref 80. Copyright 2009 The Optical Society.

of peptides and proteins can slowly assemble over time in different tissues. They can be described as linear crystals of proteinaceous units with characteristic β -sheet conformations, ⁸⁷ and their nanoscale structure can be identified using transmission electron microscopy (TEM) and atomic force microscopy (AFM). ⁸⁸ Amyloid nanofibrils are implicated in a variety of diseases exemplified by Huntington's, Alzheimer's, and Parkinson's diseases, type 2 diabetes, senility, and atrial and systemic amyloidosis. ⁸⁹ Besides being label-free, advantages of the THz spectral range for amyloid detection include the following: (i) its safety due to the nonionizing nature of photons with energies between \sim 0.001 eV and \sim 0.01 eV; (ii) resonances in the THz spectra describe not only intra-

molecular vibrational levels, but also strongly coupled intermolecular vibrations; on and (iii) THz beams may be used for the detection and dissolution of fibrous nanofibers, opening the possibility for treatment of amyloid deposits.

TCD imaging may also be promising for biomedical applications (Figure 7). THz spectroscopy is already known for its ability to differentiate human tissues such as skin and muscle, and dysplasia nevi with high sensitivity; 92,93 TCD would be expected to enhance imaging contrast as most tissues have chiral structures or at least those related to asymmetric shapes and structural changes. Visualization of basal cell skin cancer was achieved by a THz imaging system based on the difference between the absorption coefficients of cancerous

and normal tissues, ⁹⁴ and the system also identified tumors in mammary glands, lungs, the pancreas, and the brain. ^{95–97} Different from X-ray, which cannot distinguish left and right structural tissues, it is possible to gain medically relevant working behaviors of these using in vivo TCD imaging. It is also expected that chiral nanostructures, represented by conjugates between biomolecules and nanoparticles, can be examined by TCD imaging (Figure 8) and detection of their vibrations in various molecular and cellular environments for disease diagnosis and therapy within, for instance, human tissues is possible. ^{98,99}

Chiral Phonons, Chiral Photons, and Their Interactions. Chiral metasurfaces such as Archimedean spiral arrays, 65,100 double split-ring resonators, 101,102 and origami/kirigami structures 103 have been thoroughly investigated by TA and similar modalities of THz spectroscopy. However, the chirality in nanostructures has not been studied and one can expect numerous strong polarization phenomena that will accelerate the development of chiral photonics in the THz range. Additionally, TCD spectroscopy and polarization-resolved imaging systems offer the possibility of revealing the fundamental phenomena associated with chiral phonons, photons, and their interactions that have not yet been accessible.

One exemplary case is the observation of temperature dependence of chiral phonons in biomolecular crystals, which follows the Bose–Einstein distribution. ⁴⁸ Recently, Choi et al. ⁴⁸ found that, by using TCD spectroscopy, one of the phonon modes in L-Glu microcrystals is likely to correspond to chiral bosons. The observed gradual shift of energy at elevated temperatures fits nearly perfectly with a physical model based on Bose–Einstein condensation. Concomitantly, the complexity of phononic vibrations increases around the melting temperature, which is related to increased asymmetry of and coupling between different phononic modes related to the phase transformation. The fundamental study of chiral bosons and their spectroscopic signatures may contribute to understanding the quantum Hall effect where chirality is involved in quantum mechanics. ¹⁰⁴

The spectroscopic toolbox of chiral THz photons can also help to identify materials and reveal their properties for emerging fields such as topological insulators and perovskites. Topological edge states that are chiral have shown promising properties for integrated photonic chips because they show strong spin—orbit coupling and, therefore, unidirectional propagation of photons without back scattering. Complex heterostructures, such as layers of magnetic Weyl semimetals, which are often necessary to realize chiral edge states and TCD spectroscopy, can help to theorize a new paradigm for materials that can carry dissipation-less current and have high Curie temperatures.

Chiral Phonons in Strong Coupling Regime. Strong coupling phenomena between photons and phonons would be one of the interesting fundamental phenomena to observe. This is mainly because weak TCD and TORD signals from biomolecules could be dramatically enhanced by using conventional Fabry—Pérot cavity systems as well as plasmonic nanostructures when they are in a strong coupling regime. The process of excited state decay in the weak coupling regime and in a two-level system is determined by the Fermi golden rule. It is typically considered to be irreversible, but the coherent energy can be exchanged and bounced back between light and matter in the strong coupling regime, which is

reversible. 108 Therefore, in the strong coupling regime for the light-matter interaction, the energy states of the photons and the vibrational states of molecules form hybrid quantum states known as polaritons.⁹⁰ Recently, Damari et al. reported coherent Rabi oscillation and splitting in the THz range from α -lactose molecules using two sets of mirrors. ⁹⁰ This result indicates that the cavity mode is strongly coupled to the intermolecular vibration and modifying collective vibrational modes, and thus, polaritonic chemistry is also possible by judiciously controlled THz photons. 90 Consequently, the coupling between the circularly polarized THz beam and chiral phonon mode in biomolecules is expected to be observed and to open up new possibilities for applications of TCD spectroscopy considering their strong THz field confinement (light to volumes over 10⁶ times) and relatively long lifetimes (approximately picoseconds). Not only important for chemistry and biology, but in physics, the influence of polaritons on nontrivial spatial shaping of phonons, such as chiral phonons, is a fundamental question that could be addressed. 110

TCD of Chiral Nanostructures. THz frequency radiation can stimulate the motion of charge carrier quasiparticles (e.g., electrons and holes, surface plasmons, excitons, and polarons) for semiconducting/metallic materials and also excite collective vibrations (e.g., phonons) for crystalline materials. 111 Moreover, THz spectroscopy can measure charge carriers and phonons mentioned above but do so in a noncontact and noninvasive manner without cumbersome electron beam lithography and device processing, making the technique particularly suitable for nanostructured materials and nanodevices. These capabilities have drawn tremendous attention to applications of THz spectroscopy, such as the measurement of conductivity in nanowires; the same can be applied to TCD on chiral nanostructures exemplified by twisted nanoribbons or crystals from achiral molecules undergoing symmetry breaking due to nanoscale dimensions. 112,113 As such, we expect that the following nanostructures may be particularly interesting to explore using TCD and other polarization resolved spectroscopies in the THz range.

- (1) van der Waals heterostructures, 2D materials stacked with twisted angles, have been extensively studied because of their fascinating strongly correlated phenomena including correlated insulating states, unconventional superconductivity, and ferromagnetism. 114,115 Considering the variety of 2D materials 116,117 that can be assembled and their sensitivity of twisted angles in moiré patterns, TCD could be employed as a new spectroscopic method for studies on their nontrivial topology and electron–electron interactions. 118
- (2) Biocomposites, or biomimetic materials, where chitin molecules are often arranged into a helical arrangement, have impressive mechanical properties effectively preventing crack propagation and sustaining large impacts. The noncontact imaging capability of TCD spectroscopy and imaging modality can directly measure changing chiral phonon modes under application of mechanical stress. The relationship between mechanical properties such as Young's modulus and toughness of materials with optical properties in the THz range represents an important result that can be obtained by TCD. 120

(3) Metal-organic chiral nanostructures, formed by coordination polymerization of metal ions through organic ligands, are needed for a broad spectrum of applications including supercapacitors, ¹²¹ catalysis, ¹²² carbon capture, ¹²³ and molecular separation. ¹²⁴ Self-assembly of organic molecules and/or metal ions into nanostructures has evolved as an attractive and facile strategy for synthesizing chiral nanomaterials. Since these metalorganic chiral nanostructures have both noncovalent bonds and metallic nanoscale components, we would expect strong THz optical activity as quasiparticles transport or phonons propagate within the structures. It is already proven for amino acids or peptide directed synthesis of gold nanoparticles 125,126 and copper aspartic acid nanofibers 127 that they show high CD value with large g-factors in the UV to visible range. Of special interest is the experimental identification of topologically protected edge-modes that can be abundant in chiral nanoastructures with high contribution of cooperative coordination bonds and chiral interfaces where the edgemodes can propagate.

Near-Field TCD Imaging. Many applications of THz spectroscopy and imaging have been diffraction limited because THz wavelengths are long (\sim 300 μ m) compared to the optical and IR parts of the spectrum, leading to a relatively low spatial modulation accuracy and spatial resolution in the far-field zone to roughly $60^{\circ} \mu \text{m}$. Imaging with such resolution is considered to be insufficient for most of bio-, chemical, and electronic materials, where the analysis of molecular complexes or nanomaterials requires spatial resolutions in the nanometer scale. 129-131

Near-field THz imaging 132 breaking the diffraction limit could provide the solution to this problem (Figure 9a). Nearfield methods are able to increase spatial resolution to a few tens of nanometers by scattering a THz beam with the tip of an AFM. 132-134 Imaging individual biomolecules, single proteins, single DNA strands, and nanoparticles become possible by using a THz near-field scanning optical microscope (THz-NSOM, Figure 9b-e). While the realization of a TCD version of THz-NSOM is a future task, TCD-NSOM might reveal information inaccessible for TA measurements, including the precise orientation of molecules or particles similar to data polarization-resolved optical microscopy. 135 Another reason to realize super-resolution TCD is to better understand the structural changes of biomolecules especially when bound to water molecules or other receptors. Unlike conventional optical microscopy, THz imaging does not require luminescent labels and is not damaging to chemical structures, which makes this evaluation possible. Note that current transmissive-type far-field THz spectroscopy cannot resolve spectral signatures from a sample due to the thickness of highly absorptive water layer, broadening effect of water, and low sensitivity, which is originated from low dielectric constants of biomolecules. 133 Another challenge expected to be solved by TCD with higher resolution is heterogeneity of TCD signals including sign flipping and polarization scrambling that could arise from microscale anisotropic particles as well as edges of the sample.48 TCD super-resolution imaging could provide a straightforward approach for the resolution of structurefunction relationships for an ensemble of molecules that cannot be elucidated by current TCD spectroscopy. Spatially well-resolved TCD maps will also be essential for the

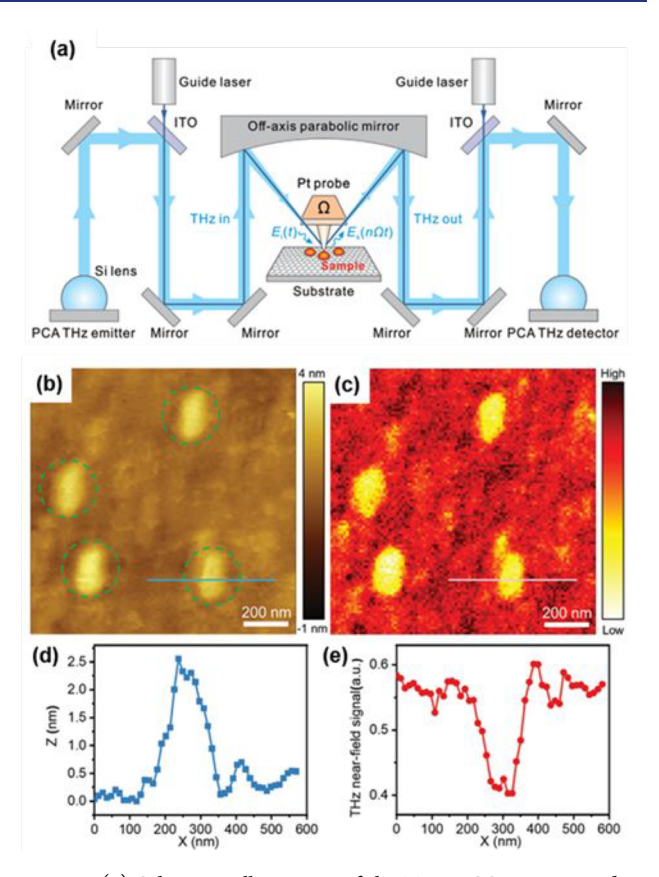


Figure 9. (a) Schematic illustration of the THz NSOM setup and its use for nanoscale materials imaging. (b) Topological AFM image of immunoglobulin G (IgG). (c) Corresponding THz-scattering map with 200 × 200 pixels. Magnitude of electric field values of the timedomain signals are reconstructed. (d and e) Cross-sectional profiles along the lines indicated in (b) and (c), respectively. Reprinted with permission from ref 133. Copyright 2020 John Wiley and Sons.

understanding of propagation of chiral phonons in nanowires and other nanostructures. Additionally they will be particularly useful for identification of topologically protected edge-modes that can be particularly abundant for chiral nanoscale structures.

TCD and Big Data Technologies. Both advantages and disadvantages of TCD spectroscopy naturally lead to the applications of rapidly developing technologies for processing large data sets obtained, for instance, by hyperspectral setups.⁴ Both the high information content and high noise levels of tradiutional THz spectra logically naturally lead to the application of machine learning (ML) for their analysis. The recent advances in this area showed that THz spectra can be accurately and automatically decoded with highly trained ML algorithms even when peaks are broad and often indistinct. 136-140 These capabilities become particularly important in biomedical fields, where chemometric ML models in data preprocessing, feature selection, and multivariate analysis improve the accuracy of disease diagnosis. 141-143

A wide range of ML methodologies have been proposed to improve computational accuracy, cost, and speed in IR, Raman, VCD, and ECD spectra (Figure 10). 145-151 Similar advances must be possible for TCD spectroscopy, too. Although there are no (to the best of our knowledge) MLbased methodologies developed and published for TCD yet, special features of this spectroscopy and its implementation for multidimensional analysis of the biological and abiological

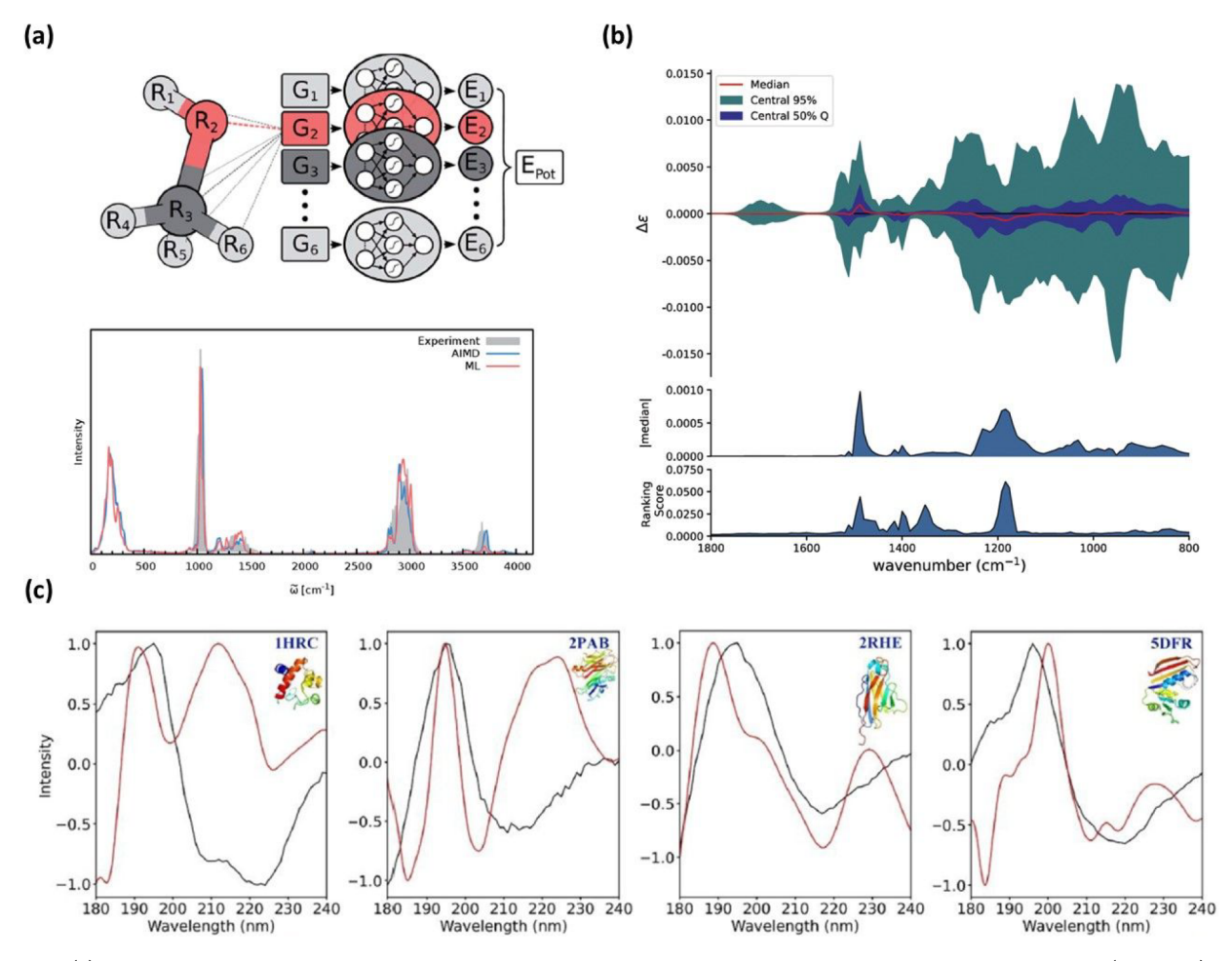


Figure 10. (a) ML-based MD simulation for IR spectra. Schematic illustration of a high-dimensional neural network potential (HDNNP) and IR spectra of methanol simulated by HDNNP and conventional ab initio MD. The Cartesian coordinates (Ri) of each atom are transformed into many-body symmetry functions (Gi) serving as inputs for neural network that derives the potential energy (E_{pot}) of the molecule. Reprinted with permission from ref 151. Copyright 2017 Royal Society of Chemistry (CC-BY 3.0). (b) ML-based simulation of VCD spectra of (+)- α -pinene. Reprinted with permission from ref 146. Copyright 2021 Royal Society of Chemistry. (c) ML-based simulation of ECD spectra of peptides predicted based on 1000 MD configurations. Reprinted with permission from ref 150. Copyright 2021 Americal Chemical Society.

structures discussed above make this spectroscopy particularly suitable for the application of ML. We can offer the reader the following reasons in support of our vision of the integration of ML and TCD for the emerging data-driven world.

- (1) TCD spectra originate from strongly coupled vibronic and phononic vibrations, which makes these spectra sensitive to small alterations of molecular structure and long-range crystalline order. Being trained on spectroscopic data for target chemicals, TCD augmented by ML algorithms will be broadly applicable as a quality control tool for complex mixtures of biochemicals. 144
- (2) Density functional theory (DFT) and molecular dynamics (MD) computations for analysis and peak recovery from TCD spectra can be laborious. They also require specific expertise that may not be available for all the TCD users. Implementation of open-access physicsbased ML algorithms trained on purposefully generated computational spectra augmented with similarly large library of experimental ones can be utilized by general users for data analysis. The same methodology can also be advantageous for prediction of TCD spectra for various chiral organic, inorganic, and hybrid inorganic—

- organic crystals 152,153 and uncovering their TCD fingerprints.
- (3) As the complexity and diversity of intermolecular interactions increase, the noise in the data stream is likely to increase as well. We expect that ML denoising will be common to overcome common interference from water absorption.

CONCLUSIONS

The development of TCD spectroscopy is described in this Perspective starting from its theoretical foundations and initial observations in biomolecule assemblies, to experimental methodologies and metamaterials-enabled hardware. Advancement in TCD will require further elaboration of complex coupled long-range vibrations in chiral materials and at their interfaces, where topological effects can be present. Implementation of ML technologies will further facilitate interpretation of TCD fingerprints of multiple organic, inorganic, and hybrid materials. We expect that these advances will engender multiple applications of TCD emerging from its high information content of TCD spectra and nondestructive and nonionizing nature of this spectroscopy making it potentially safe to its broad use. Special attention was given to chiral

phonons in nanomaterials and biomolecules revealed by TCD spectroscopy. Observation and modulation of chiral phonons can be of interest for medical, optoelectronic, ¹⁵⁴ computational, ¹⁵⁵ and sustainability ¹⁵⁶ technologies.

TERMINOLOGY

- Exciton: A bound state of an electron and a hole pair attracted with Coulomb force
- Phonon: A discrete unit of vibrations in a crystal lattice
- Photon: An elementary particle of electromagnetic field/ radiation
- Plasmon: A quantized particle of plasma oscillation
- Polariton: A hybridized particle resulting from a strong coupling between photon and an electric dipole
- Vibronic: Originates from the combination of the terms "vibrational" and "electronic", denoting the idea that in a molecule, vibrational and electronic interactions are interrelated and influence each other.

AUTHOR INFORMATION

Corresponding Author

Nicholas A. Kotov — Biointerfaces Institute, University of Michigan, Ann Arbor, Michigan 48109, United States; Department of Chemical Engineering, Department of Biomedical Engineering, and Program in Macromolecular Science and Engineering, University of Michigan, Ann Arbor, Michigan 48109, United States; orcid.org/0000-0002-6864-5804; Email: kotov@umich.edu

Authors

Won Jin Choi — Biointerfaces Institute, University of Michigan, Ann Arbor, Michigan 48109, United States; Department of Chemical Engineering, University of Michigan, Ann Arbor, Michigan 48109, United States; Physical and Life Sciences, Lawrence Livermore National Laboratory, Livermore, California 94550, United States; orcid.org/0000-0001-6303-8899

Sang Hyun Lee — Biointerfaces Institute, University of Michigan, Ann Arbor, Michigan 48109, United States; Department of Electrical Engineering and Computer Science, University of Michigan, Ann Arbor, Michigan 48109, United States

Bum Chul Park — Biointerfaces Institute, University of Michigan, Ann Arbor, Michigan 48109, United States; Department of Chemical Engineering, University of Michigan, Ann Arbor, Michigan 48109, United States

Complete contact information is available at: https://pubs.acs.org/10.1021/jacs.2c04817

Funding

This work was supported by Vannevar Bush DoD Fellowship to N.A.K. titled "Engineered Chiral Ceramics" ONR N000141812876. This work was supported in part by the MURI project Office of Naval Research, MURI N00014-20-1-2479. N.A.K. were supported by Office of Naval Research Multidisciplinary University Research Initiative Award ONR N00014-18-1-2497. The research on TCD was also supported in part by COVID-19 Newton Award "Pathways to Complexity with Imperfect' Nanoparticles" HQ00342010033, AFOSR FA9550-20-1-0265, Graph Theory Description of Network Material and by DARPA Electromagnetic Processes and Normal Modes in Bacterial Biofilms, HR00111720067. This work was

performed under the auspices of the U.S. Department of Energy by Lawrence Livermore National Laboratory under Contract DE-AC52-07NA27344. W.J.C. gratefully acknowledge the LLNL LDRD Program for funding support of this project under No. 22-ERD-056.

Notes

The authors declare no competing financial interest.

ACKNOWLEDGMENTS

The authors are grateful to Dr. Gong Cheng, Yifan Shen, and Prof. Theodore Norris for fruitful discussions about THz spectroscopy of biomaterials.

REFERENCES

- (1) Crosby, J. Synthesis of Optically Active Compounds: A Large Scale Perspective. *Tetrahedron* **1991**, 47 (27), 4789–4846.
- (2) Kasprzyk-Hordern, B. Pharmacologically Active Compounds in the Environment and Their Chirality. *Chem. Soc. Rev.* **2010**, *39* (11), 4466–4503.
- (3) Jawiczuk, M.; Górecki, M.; Masnyk, M.; Frelek, J. Complementarity of Electronic and Vibrational Circular Dichroism Based on Stereochemical Studies of Vic-Diols. *TrAC Trends Anal. Chem.* **2015**, 73, 119–128.
- (4) Mándi, A.; Kurtán, T. Applications of OR/ECD/VCD to the Structure Elucidation of Natural Products. *Nat. Prod. Rep.* **2019**, *36* (6), 889–918.
- (5) Choi, W. J.; Cheng, G.; Huang, Z.; Zhang, S.; Norris, T. B.; Kotov, N. A. Terahertz Circular Dichroism Spectroscopy of Biomaterials Enabled by Kirigami Polarization Modulators. *Nat. Mater.* **2019**, *18*, 820–826.
- (6) Kumar, J.; Nakashima, T.; Kawai, T. Circularly Polarized Luminescence in Chiral Molecules and Supramolecular Assemblies. *J. Phys. Chem. Lett.* **2015**, *6* (17), 3445–3452.
- (7) Kim, Y. H.; Zhai, Y.; Gaulding, E. A.; Habisreutinger, S. N.; Moot, T.; Rosales, B. A.; Lu, H.; Hazarika, A.; Brunecky, R.; Wheeler, L. M.; Berry, J. J.; Beard, M. C.; Luther, J. M. Strategies to Achieve High Circularly Polarized Luminescence from Colloidal Organic-Inorganic Hybrid Perovskite Nanocrystals. *ACS Nano* **2020**, *14* (7), 8816–8825.
- (8) Deng, Y.; Wang, M.; Zhuang, Y.; Liu, S.; Huang, W.; Zhao, Q. Circularly Polarized Luminescence from Organic Micro-/Nano-Structures. *Light Sci. Appl.* **2021**, *10* (1), 1–18.
- (9) Hiramatsu, K.; Leproux, P.; Couderc, V.; Nagata, T.; Kano, H. Raman Optical Activity Spectroscopy by Visible-Excited Coherent Anti-Stokes Raman Scattering. *Opt. Lett.* **2015**, *40* (17), 4170.
- (10) Sun, M.; Zhang, Z.; Wang, P.; Li, Q.; Ma, F.; Xu, H. Remotely Excited Raman Optical Activity Using Chiral Plasmon Propagation in Ag Nanowires. *Light Sci. Appl.* **2013**, 2 (11), e112–e112.
- (11) Lombardini, R.; Acevedo, R.; Halas, N. J.; Johnson, B. R. Plasmonic Enhancement of Raman Optical Activity in Molecules near Metal Nanoshells: Theoretical Comparison of Circular Polarization Methods. J. Phys. Chem. C 2010, 114 (16), 7390–7400.
- (12) Kurouski, D. Advances of Vibrational Circular Dichroism (VCD) in Bioanalytical Chemistry. A Review. *Anal. Chim. Acta* **2017**, 990, 54–66.
- (13) Fischer, P.; Hache, F. Nonlinear Optical Spectroscopy of Chiral Molecules. *Chirality* **2005**, *17* (8), 421–437.
- (14) Collins, J. T.; Rusimova, K. R.; Hooper, D. C.; Jeong, H. H.; Ohnoutek, L.; Pradaux-Caggiano, F.; Verbiest, T.; Carbery, D. R.; Fischer, P.; Valev, V. K. First Observation of Optical Activity in Hyper-Rayleigh Scattering. *Phys. Rev. X* **2019**, *9* (1), 11024.
- (15) Ohnoutek, L.; Kim, J. Y.; Lu, J.; Olohan, B. J.; Răsădean, D. M.; Dan Pantoş, G.; Kotov, N. A.; Valev, V. K. Third-Harmonic Mie Scattering from Semiconductor Nanohelices. *Nat. Photonics* **2022**, *16*, 126–133.
- (16) Verreault, D.; Moreno, K.; Merlet, É.; Adamietz, F.; Kauffmann, B.; Ferrand, Y.; Olivier, C.; Rodriguez, V. Hyper-Rayleigh Scattering

- as a New Chiroptical Method: Uncovering the Nonlinear Optical Activity of Aromatic Oligoamide Foldamers. *J. Am. Chem. Soc.* **2020**, 142 (1), 257–263.
- (17) Van Cleuvenbergen, S.; Asselberghs, I.; Vanormelingen, W.; Verbiest, T.; Franz, E.; Clays, K.; Kuzyk, M. G.; Koeckelberghs, G. Record-High Hyperpolarizabilities in Conjugated Polymers. *J. Mater. Chem. C* **2014**, 2 (23), 4533–4538.
- (18) Botek, E.; Spassova, M.; Champagne, B.; Asselberghs, I.; Persoons, A.; Clays, K. Hyper-Rayleigh Scattering of Neutral and Charged Helicenes. *Chem. Phys. Lett.* **2005**, *412* (4–6), 274–279.
- (19) Okuno, M.; Ishibashi, T. Heterodyne-Detected Achiral and Chiral Vibrational Sum Frequency Generation of Proteins at Air/Water Interface. *J. Phys. Chem. C* **2015**, *119* (18), 9947–9954.
- (20) Petralli-Mallow, T.; Wong, T. M.; Byers, J. D.; Yee, H. I.; Hicks, J. M. Circular Dichroism Spectroscopy at Interfaces: A Surface Second Harmonic Generation Study. *J. Phys. Chem.* **1993**, 97, 1383–1388.
- (21) Russier-Antoine, I.; Bertorelle, F.; Kulesza, A.; Soleilhac, A.; Bensalah-Ledoux, A.; Guy, S.; Dugourd, P.; Brevet, P. F.; Antoine, R. Chiral Supramolecular Gold-Cysteine Nanoparticles: Chiroptical and Nonlinear Optical Properties. *Prog. Nat. Sci. Mater. Int.* **2016**, *26* (5), 455–460.
- (22) Wang, Z.; Fu, L.; Ma, G.; Yan, E. C. Y. Broad-Bandwidth Chiral Sum Frequency Generation Spectroscopy for Probing the Kinetics of Proteins at Interfaces. *Langmuir* **2015**, *31* (42), 11384–11398.
- (23) Ohnoutek, L.; Jeong, H. H.; Jones, R. R.; Sachs, J.; Olohan, B. J.; Răsădean, D. M.; Pantoş, G. D.; Andrews, D. L.; Fischer, P.; Valev, V. K. Optical Activity in Third-Harmonic Rayleigh Scattering: A New Route for Measuring Chirality. *Laser Photonics Rev.* **2021**, *15* (11), 2100235
- (24) Peleg, G.; Lewis, A.; Bouevitch, O.; Loew, L.; Parnas, D.; Linial, M. Gigantic Optical Non-Linearities from Nanoparticle-Enhanced Molecular Probes with Potential for Selectively Imaging the Structure and Physiology of Nanometric Regions in Cellular Systems. *Bioimaging* 1996, 4 (3), 215–224.
- (25) Probst, P. T.; Mayer, M.; Gupta, V.; Steiner, A. M.; Zhou, Z.; Auernhammer, G. K.; König, T. A. F.; Fery, A. Mechano-Tunable Chiral Metasurfaces via Colloidal Assembly. *Nat. Mater.* **2021**, *20*, 1024–1028.
- (26) Ohnoutek, L.; Cho, N. H.; Allen Murphy, A. W.; Kim, H.; Rǎsǎdean, D. M.; Pantoş, G. D.; Nam, K. T.; Valev, V. K. Single Nanoparticle Chiroptics in a Liquid: Optical Activity in Hyper-Rayleigh Scattering from Au Helicoids. *Nano Lett.* **2020**, *20* (8), 5792–5798.
- (27) Chuntonov, L.; Haran, G. Maximal Raman Optical Activity in Hybrid Single Molecule-Plasmonic Nanostructures with Multiple Dipolar Resonances. *Nano Lett.* **2013**, *13* (3), 1285–1290.
- (28) Kim, K. H.; Chae, S. S.; Jang, S.; Choi, W. J.; Chang, H.; Lee, J. O.; Lee, T., Il Atomic Force Masking" Induced Formation of Effective Hot Spots along Grain Boundaries of Metal Thin Films. *ACS Appl. Mater. Interfaces* **2016**, *8* (47), 32094–32101.
- (29) Yan, J.; Feng, W.; Kim, J. Y.; Lu, J.; Kumar, P.; Mu, Z.; Wu, X.; Mao, X.; Kotov, N. A. Self-Assembly of Chiral Nanoparticles into Semiconductor Helices with Tunable near-Infrared Optical Activity. *Chem. Mater.* **2020**, 32 (1), 476–488.
- (30) Mernea, M.; Calborean, O.; Grigore, O.; Dascalu, T.; Mihailescu, D. F. Validation of Protein Structural Models Using THz Spectroscopy: A Promising Approach to Solve Three-Dimensional Structures. *Opt. Quantum Electron.* **2014**, *46* (4), 505–514.
- (31) González-Jiménez, M.; Ramakrishnan, G.; Harwood, T.; Lapthorn, A. J.; Kelly, S. M.; Ellis, E. M.; Wynne, K. Observation of Coherent Delocalized Phonon-like Modes in DNA under Physiological Conditions. *Nat. Commun.* **2016**, *7*, 11799.
- (32) Rutz, F.; Koch, M.; Khare, S.; Moneke, M.; Richter, H.; Ewert, U. Terahertz Quality Control of Polymeric Products. *Int. J. Infrared Millimeter Waves* **2006**, *27* (4), 547–556.
- (33) Heo, C.; Ha, T.; You, C.; Huynh, T.; Lim, H.; Kim, J.; Kesama, M. R.; Lee, J.; Kim, T.-T.; Lee, Y. H. Identifying Fibrillization State of

- $A\beta$ Protein via Near-Field THz Conductance Measurement. ACS Nano 2020, 14 (6), 6548-6558.
- (34) Plusquellic, D. F.; Siegrist, K.; Heilweil, E. J.; Esenturk, O. Applications of Terahertz Spectroscopy in Biosystems. *ChemPhysChem* **2007**, *8* (17), 2412–2431.
- (35) Yang, X.; Zhao, X.; Yang, K.; Liu, Y.; Liu, Y.; Fu, W.; Luo, Y. Biomedical Applications of Terahertz Spectroscopy and Imaging. *Trends Biotechnol.* **2016**, 34 (10), 810–824.
- (36) Pawar, A. Y.; Sonawane, D. D.; Erande, K. B.; Derle, D. V. Terahertz Technology and Its Applications. *Drug Invent. Today* **2013**, 5 (2), 157–163.
- (37) Puc, U.; Abina, A.; Jeglič, A.; Zidanšek, A.; Kašalynas, I.; Venckevičius, R.; Valušis, G. Spectroscopic Analysis of Melatonin in the Terahertz Frequency Range. Sensors (Basel). 2018, 18 (12), 4098.
- (38) Allis, D. G.; Korter, T. M. Theoretical Analysis of the Terahertz Spectrum of the High Explosive PETN. *ChemPhysChem* **2006**, 7 (11), 2398–2408.
- (39) Mattana, S.; Caponi, S.; Tamagnini, F.; Fioretto, D.; Palombo, F. Viscoelasticity of Amyloid Plaques in Transgenic Mouse Brain Studied by Brillouin Microspectroscopy and Correlative Raman Analysis. *J. Innov. Opt. Health Sci.* **2017**, *10* (06), 1742001.
- (40) D'Angelo, G.; Conti Nibali, V.; Crupi, C.; Rifici, S.; Wanderlingh, U.; Paciaroni, A.; Sacchetti, F.; Branca, C. Probing Intermolecular Interactions in Phospholipid Bilayers by Far-Infrared Spectroscopy. *J. Phys. Chem. B* **2017**, *121* (6), 1204–1210.
- (41) Wittlin, A.; Genzel, L.; Kremer, F.; Häseler, S.; Poglitsch, A.; Rupprecht, A. Far-Infrared Spectroscopy on Oriented Films of Dry and Hydrated DNA. *Phys. Rev. A* **1986**, 34 (1), 493–500.
- (42) Tang, M.; Huang, Q.; Wei, D.; Zhao, G.; Chang, T.; Kou, K.; Wang, M.; Du, C.; Fu, W.; Cui, H.-L. Terahertz Spectroscopy of Oligonucleotides in Aqueous Solutions. *J. Biomed. Opt.* **2015**, 20 (9), 095009.
- (43) Lvovska, M. I.; Seeman, N. C.; Sha, R.; Globus, T. R.; Khromova, T. B.; Dorofeeva, T. S. THz Characterization of DNA Four-Way Junction and Its Components. *IEEE Trans. Nanotechnol.* **2010**, 9 (5), 610–617.
- (44) Zhang, F.; Wang, H. W.; Tominaga, K.; Hayashi, M.; Hasunuma, T.; Kondo, A. Application of THz Vibrational Spectroscopy to Molecular Characterization and the Theoretical Fundamentals: An Illustration Using Saccharide Molecules. *Chem. An Asian J.* **2017**, *12* (3), 324–331.
- (45) Van Dijk, L.; Bobbert, P. A.; Spano, F. C. Extreme Sensitivity of Circular Dichroism to Long-Range Excitonic Couplings in Helical Supramolecular Assemblies. *J. Phys. Chem. B* **2010**, *114* (2), 817–825.
- (46) Markelz, A.; Whitmire, S.; Hillebrecht, J.; Birge, R. THz Time Domain Spectroscopy of Biomolecular Conformational Modes. *Phys. Med. Biol.* **2002**, *47* (21), 3797–3805.
- (47) Ebbinghaus, S.; Seung, J. K.; Heyden, M.; Yu, X.; Gruebele, M.; Leitner, D. M.; Havenith, M. Protein Sequence- and PH-Dependent Hydration Probed by Terahertz Spectroscopy. *J. Am. Chem. Soc.* **2008**, 130 (8), 2374–2375.
- (48) Choi, W. J.; Yano, K.; Cha, M.; Colombari, F. M.; Kim, J. Y.; Wang, Y.; Lee, S. H.; Sun, K.; Kruger, J. M.; de Moura, A. F.; Kotov, N. A. Chiral Phonons in Microcrystals and Nanofibrils of Biomolecules. *Nat. Photonics* **2022**, *16*, 366–373.
- (49) Choi, W. Reconfigurable Kirigami Optics and Chiral Phonons, Ph.D. Dissertation, University of Michigan, Ann Arbor, MI, 2021. DOI: 10.7302/1473 (accessed 2022-07-21).
- (50) Zhu, H.; Yi, J.; Li, M. Y.; Xiao, J.; Zhang, L.; Yang, C. W.; Kaindl, R. A.; Li, L. J.; Wang, Y.; Zhang, X. Observation of Chiral Phonons. *Science* **2018**, 359 (6375), 579–582.
- (51) Chen, X.; Lu, X.; Dubey, S.; Yao, Q.; Liu, S.; Wang, X.; Xiong, Q.; Zhang, L.; Srivastava, A. Entanglement of Single-Photons and Chiral Phonons in Atomically Thin WSe2. *Nat. Phys.* **2019**, *15*, 221–227.
- (52) Rogers, D. M.; Jasim, S. B.; Dyer, N. T.; Auvray, F.; Réfrégiers, M.; Hirst, J. D. Electronic Circular Dichroism Spectroscopy of Proteins. *Chem.* **2019**, *5* (11), 2751–2774.

- (53) Kurouski, D. Advances of Vibrational Circular Dichroism (VCD) in Bioanalytical Chemistry. A Review. *Anal. Chim. Acta* **2017**, 990, 54–66.
- (54) Liu, R.; He, M.; Su, R.; Yu, Y.; Qi, W.; He, Z. Insulin Amyloid Fibrillation Studied by Terahertz Spectroscopy and Other Biophysical Methods. *Biochem. Biophys. Res. Commun.* **2010**, 391 (1), 862–867.
- (55) Zhu, L.; Zou, Y.; Li, J.; Liu, Q. Terahertz Spectroscopy of Neurodegenerative Diseases: The Correlation between Terahertz Biophysics and Pathological Analysis. *Opt. InfoBase Conf. Pap.* **2018**, 9–11.
- (56) Xu, J.; Ramian, G. J.; Galan, J. F.; Savvidis, P. G.; Scopatz, A. M.; Birge, R. R.; Allen, S. J.; Plaxco, K. W. Terahertz Circular Dichroism Spectroscopy: A Potential Approach to the in Situ Detection of Life's Metabolic and Genetic Machinery. *Astrobiology* **2003**, *3* (3), 489–504.
- (57) Choi, J. H.; Cho, M. Terahertz Chiroptical Spectroscopy of an α -Helical Polypeptide: A Molecular Dynamics Simulation Study. *J. Phys. Chem. B* **2014**, *118* (45), 12837–12843.
- (58) Keiderling, T. A. Instrumentation for Vibrational Circular Dichroism Spectroscopy: Method Comparison and Newer Developments. *Molecules* **2018**, 23 (9), 2404.
- (59) Lewis, R. A. A Review of Terahertz Detectors. J. Phys. D. Appl. Phys. 2019, 52 (43), 433001.
- (60) Cheng, G.; Choi, W. J.; Jang, H.-J.; Kotov, N. A.; Norris, T. B. Terahertz Time-Domain Polarimetry for Generalized Anistropic and Chiral Materials. In *Proceedings of SPIE The International Society for Optical Engineering*; **2019**; Vol. 10917. DOI: 10.1117/12.2516383.
- (61) Neu, J.; Schmuttenmaer, C. A. Tutorial: An Introduction to Terahertz Time Domain Spectroscopy (THz-TDS). *J. Appl. Phys.* **2018**, *124* (23), 231101.
- (62) Miyamaru, F.; Kondo, T.; Nagashima, T.; Hangyo, M. Large Polarization Change in Two-Dimensional Metallic Photonic Crystals in Subterahertz Region. *Appl. Phys. Lett.* **2003**, 82 (16), 2568–2570.
- (63) Singh, R.; Plum, E.; Zhang, W.; Zheludev, N. I. Highly Tunable Optical Activity in Planar Achiral Terahertz Metamaterials. *Opt. Express* **2010**, *18* (13), 13425.
- (64) Neu, J.; Aschaffenburg, D. J.; Williams, M. R. C.; Schmuttenmaer, C. A. Optimization of Terahertz Metamaterials for Near-Field Sensing of Chiral Substances. *IEEE Trans. Terahertz Sci. Technol.* **2017**, *7* (6), 755–764.
- (65) Kan, T.; Isozaki, A.; Kanda, N.; Nemoto, N.; Konishi, K.; Takahashi, H.; Kuwata-Gonokami, M.; Matsumoto, K.; Shimoyama, I. Enantiomeric Switching of Chiral Metamaterial for Terahertz Polarization Modulation Employing Vertically Deformable MEMS Spirals. *Nat. Commun.* **2015**, *6*, 8422.
- (66) Deng, Y.; McKinney, J. A.; George, D. K.; Niessen, K. A.; Sharma, A.; Markelz, A. G. Near-Field Stationary Sample Terahertz Spectroscopic Polarimetry for Biomolecular Structural Dynamics Determination. *ACS Photonics* **2021**, *8* (2), 658–668.
- (67) Kanda, N.; Konishi, K.; Kuwata-Gonokami, M. Terahertz Wave Polarization Rotation with Double Layered Metal Grating of Complimentary Chiral Patterns. *Opt. Express* **2007**, *15* (18), 11117.
- (68) Nagashima, T.; Tani, M.; Hangyo, M. Polarization-Sensitive THz-TDS and Its Application to Anisotropy Sensing. *J. Infrared, Millimeter, Terahertz Waves* **2013**, 34 (11), 740–775.
- (69) Kawada, Y.; Yasuda, T.; Nakanishi, A.; Akiyama, K.; Hakamata, K.; Takahashi, H. Achromatic Prism-Type Wave Plate for Broadband Terahertz Pulses. *Opt. Lett.* **2014**, *39* (9), 2794.
- (70) McDonnell, C.; Deng, J.; Sideris, S.; Ellenbogen, T.; Li, G. Functional THz Emitters Based on Pancharatnam-Berry Phase Nonlinear Metasurfaces. *Nat. Commun.* **2021**, *12*, 30.
- (71) Williams, M. R. C.; True, A. B.; Izmaylov, A. F.; French, T. A.; Schroeck, K.; Schmuttenmaer, C. A. Terahertz Spectroscopy of Enantiopure and Racemic Polycrystalline Valine. *Phys. Chem. Chem. Phys.* **2011**, *13* (24), 11719–11730.
- (72) Korter, T. M.; Balu, R.; Campbell, M. B.; Beard, M. C.; Gregurick, S. K.; Heilweil, E. J. Terahertz Spectroscopy of Solid Serine and Cysteine. *Chem. Phys. Lett.* **2006**, *418* (1–3), 65–70.

- (73) Williams, M. R. C.; Aschaffenburg, D. J.; Ofori-Okai, B. K.; Schmuttenmaer, C. A. Intermolecular Vibrations in Hydrophobic Amino Acid Crystals: Experiments and Calculations. *J. Phys. Chem. B* **2013**, *117* (36), 10444–10461.
- (74) Hamada, D.; Dobson, C. M. A Kinetic Study of Beta-Lactoglobulin Amyloid Fibril Formation Promoted by Urea. *Protein Sci.* **2002**, *11* (10), 2417–2426.
- (75) Leonov, D. V.; Dzuba, S. A.; Surovtsev, N. V. Normal Vibrations of Ternary DOPC/DPPC/Cholesterol Lipid Bilayers by Low-Frequency Raman Spectroscopy. *RSC Adv.* **2019**, *9* (59), 34451–34456.
- (76) Zhang, L.; Niu, Q. Chiral Phonons at High-Symmetry Points in Monolayer Hexagonal Lattices. *Phys. Rev. Lett.* **2015**, *115*, 115502.
- (77) Liu, Y.; Lian, C. S.; Li, Y.; Xu, Y.; Duan, W. Pseudospins and Topological Effects of Phonons in a Kekulé Lattice. *Phys. Rev. Lett.* **2017**, *119*, 255901.
- (78) Yeom, J.; Santos, U. S. S.; Chekini, M.; Cha, M.; de Moura, A. F.; Kotov, N. A. A. Chiromagnetic Nanoparticles and Gels. *Science* **2018**, 359 (6371), 309–314.
- (79) Chen, H.; Wu, W.; Zhu, J.; Yang, S. A.; Zhang, L. Propagating Chiral Phonons in Three-Dimensional Materials. *Nano Lett.* **2021**, *21* (7), 3060–3065.
- (80) Oh, S. J.; Kang, J.; Maeng, I.; Suh, J.-S.; Huh, Y.-M.; Haam, S.; Son, J.-H. Nanoparticle-Enabled Terahertz Imaging for Cancer Diagnosis. *Opt. Express* **2009**, *17* (5), 3469.
- (81) Son, J.-H.; Oh, J.; Cheon, H. Potential Clinical Applications of Terahertz Radiation. *J. Appl. Phys.* **2019**, *125*, 190901.
- (82) Xiong, R.; Luan, J.; Kang, S.; Ye, C.; Singamaneni, S.; Tsukruk, V. V. Biopolymeric Photonic Structures: Design, Fabrication, and Emerging Applications. *Chem. Soc. Rev.* **2020**, 49 (3), 983–1031.
- (83) Tokunaga, E.; Yamamoto, T.; Ito, E.; Shibata, N. Understanding the Thalidomide Chirality in Biological Processes by the Self-Disproportionation of Enantiomers. Sci. Rep. 2018, 8 (1), 6–12.
- (84) Smith, S. W. Chiral Toxicology: It's the Same Thing...Only Different. *Toxicol. Sci.* **2009**, *110* (1), 4–30.
- (85) Ito, T.; Ando, H.; Suzuki, T.; Ogura, T.; Hotta, K.; Imamura, Y.; Yamaguchi, Y.; Handa, H. Identification of a Primary Target of Thalidomide Teratogenicity. *Science* **2010**, *327* (5971), 1345–1350.
- (86) Darji, M. A.; Lalge, R. M.; Marathe, S. P.; Mulay, T. D.; Fatima, T.; Alshammari, A.; Lee, H. K.; Repka, M. A.; Narasimha Murthy, S. Excipient Stability in Oral Solid Dosage Forms: A Review. *AAPS PharmSciTech* **2018**, *19* (1), 12–26.
- (87) Petkova, A. T.; Ishii, Y.; Balbach, J. J.; Antzutkin, O. N.; Leapman, R. D.; Delaglio, F.; Tycko, R. A Structural Model for Alzheimer's Beta -Amyloid Fibrils Based on Experimental Constraints from Solid State NMR. *Proc. Natl. Acad. Sci. U. S. A.* **2002**, 99 (26), 16742–16747.
- (88) Yoo, S. Il; Yang, M.; Brender, J. R.; Subramanian, V.; Sun, K.; Joo, N. E.; Jeong, S.-H.; Ramamoorthy, A.; Kotov, N. A. Inhibition of Amyloid Peptide Fibrillation by Inorganic Nanoparticles: Functional Similarities with Proteins. *Angew. Chem., Int. Ed.* **2011**, *50* (22), 5110–5115.
- (89) Enqvist, S.; Peng, S.; Persson, A.; Westermark, P. Senile Amyloidoses Diseases of Increasing Importance. *Acta Histochem.* **2003**, *105* (4), 377–378.
- (90) Damari, R.; Weinberg, O.; Krotkov, D.; Demina, N.; Akulov, K.; Golombek, A.; Schwartz, T.; Fleischer, S. Strong Coupling of Collective Intermolecular Vibrations in Organic Materials at Terahertz Frequencies. *Nat. Commun.* **2019**, *10*, 3248.
- (91) Kawasaki, T.; Tsukiyama, K.; Irizawa, A. Dissolution of a Fibrous Peptide by Terahertz Free Electron Laser. *Sci. Rep.* **2019**, 9 (1), 10636.
- (92) Zhang, R.; He, Y.; Liu, K.; Zhang, L.; Zhang, S.; Pickwell-MacPherson, E.; Zhao, Y.; Zhang, C. Composite Multiscale Entropy Analysis of Reflective Terahertz Signals for Biological Tissues. *Opt. Express* **2017**, 25 (20), 23669.
- (93) Zaytsev, K. I.; Kudrin, K. G.; Karasik, V. E.; Reshetov, I. V.; Yurchenko, S. O. In Vivo Terahertz Spectroscopy of Pigmentary Skin

- Nevi: Pilot Study of Non-Invasive Early Diagnosis of Dysplasia. *Appl. Phys. Lett.* **2015**, *106*, 053702.
- (94) Wallace, V. P.; Woodward, R. M.; Fitzgerald, A. J.; Pickwell, E.; Pye, R. J.; Arnone, D. D. Terahertz-Pulsed Imaging of Cancers. *Lasers Surg. Adv. Charact. Ther. Syst. XIII* **2003**, 4949 (September 2003), 353.
- (95) Fitzgerald, A. J. Classification of Terahertz-Pulsed Imaging Data from Excised Breast Tissue. *J. Biomed. Opt.* **2012**, *17* (1), 016005.
- (96) Brun, M. A.; Formanek, F.; Yasuda, A.; Sekine, M.; Ando, N.; Eishii, Y. Terahertz Imaging Applied to Cancer Diagnosis. *Phys. Med. Biol.* **2010**, *55* (16), 4615–4623.
- (97) Yamaguchi, S.; Fukushi, Y.; Kubota, O.; Itsuji, T.; Ouchi, T.; Yamamoto, S. Brain Tumor Imaging of Rat Fresh Tissue Using Terahertz Spectroscopy. *Sci. Rep.* **2016**, *6*, 6–11.
- (98) Smith, B. R.; Gambhir, S. S. Nanomaterials for in Vivo Imaging. *Chem. Rev.* **2017**, *117* (3), 901–986.
- (99) Gautier, C.; Bieri, M.; Dolamic, I.; Angeloni, S.; Boudon, J.; Bürgi, T. Probing Chiral Nanoparticles and Surfaces by Infrared Spectroscopy. *Chimia (Aarau)*. **2006**, *60* (11), 777–782.
- (100) Aschaffenburg, D. J.; Williams, M. R. C.; Schmuttenmaer, C. A. Terahertz Spectroscopic Polarimetry of Generalized Anisotropic Media Composed of Archimedean Spiral Arrays: Experiments and Simulations. *J. Chem. Phys.* **2016**, *144*, 174705.
- (101) Lin, Y. S.; Qian, Y.; Ma, F.; Liu, Z.; Kropelnicki, P.; Lee, C. Development of Stress-Induced Curved Actuators for a Tunable THz Filter Based on Double Split-Ring Resonators. *Appl. Phys. Lett.* **2013**, 102, 111908.
- (102) Kenanakis, G.; Zhao, R.; Stavrinidis, A.; Konstantinidis, G.; Katsarakis, N.; Kafesaki, M.; Soukoulis, C. M.; Economou, E. N. Flexible Chiral Metamaterials in the Terahertz Regime: A Comparative Study of Various Designs. *Opt. Mater. Express* **2012**, 2 (12), 1702.
- (103) Wang, Z.; Jing, L.; Yao, K.; Yang, Y.; Zheng, B.; Soukoulis, C. M.; Chen, H.; Liu, Y. Origami-Based Reconfigurable Metamaterials for Tunable Chirality. *Adv. Mater.* **2017**, *29*, 1700412.
- (104) Bracken, P. Links between the Quantum Hall Effect, Chiral Boson Theories and String Theory. *Int. J. Mod. Phys. E* **2004**, *13* (5), 961–971.
- (105) Howard, S.; Jiao, L.; Wang, Z.; Morali, N.; Batabyal, R.; Kumar-Nag, P.; Avraham, N.; Beidenkopf, H.; Vir, P.; Liu, E.; Shekhar, C.; Felser, C.; Hughes, T.; Madhavan, V. Evidence for One-Dimensional Chiral Edge States in a Magnetic Weyl Semimetal Co3Sn2S2. *Nat. Commun.* **2021**, *12*, 4269.
- (106) Parappurath, N.; Alpeggiani, F.; Kuipers, L.; Verhagen, E. Direct Observation of Topological Edge States in Silicon Photonic Crystals: Spin, Dispersion, and Chiral Routing. *Sci. Adv.* **2020**, *6* (10), No. eaaw4137.
- (107) Törma, P.; Barnes, W. L. Strong Coupling between Surface Plasmon Polaritons and Emitters: A Review. *Rep. Prog. Phys.* **2015**, 78, 013901.
- (108) Zanotto, S. Weak Coupling, Strong Coupling, Critical Coupling and Fano Resonances: A Unifying Vision. In *Springer Series in Optical Sciences*; Springer Verlag: 2018; Vol. 219, pp 551–570. DOI: 10.1007/978-3-319-99731-5_23.
- (109) Bylinkin, A.; Schnell, M.; Autore, M.; Calavalle, F.; Li, P.; Taboada-Gutièrrez, J.; Liu, S.; Edgar, J. H.; Casanova, F.; Hueso, L. E.; Alonso-Gonzalez, P.; Nikitin, A. Y.; Hillenbrand, R. Real-Space Observation of Vibrational Strong Coupling between Propagating Phonon Polaritons and Organic Molecules. *Nat. Photonics* **2021**, *15*, 197–202.
- (110) Rivera, N.; Coulter, J.; Christensen, T.; Narang, P. Ab Initio Calculation of Phonon Polaritons in Silicon Carbide and Boron Nitride. 2018, Aug 31, arxiv (optics) 1809.00058. https://arxiv.org/abs/1809.00058 (accessed 2022-11-09).
- (111) Joyce, H. J.; Boland, J. L.; Davies, C. L.; Baig, S. A.; Johnston, M. B. A Review of the Electrical Properties of Semiconductor Nanowires: Insights Gained from Terahertz Conductivity Spectroscopy. *Semicond. Sci. Technol.* **2016**, *31*, 103003.

- (112) Shtukenberg, A. G.; Punin, Y. O.; Gujral, A.; Kahr, B. Growth Actuated Bending and Twisting of Single Crystals. *Angew. Chem., Int. Ed.* **2014**, *53* (3), *672–699*.
- (113) Efrati, E. Geometric Frustration in Molecular Crystals. Isr. J. Chem. 2020, 60, 1185–1189.
- (114) Cao, Y.; Fatemi, V.; Fang, S.; Watanabe, K.; Taniguchi, T.; Kaxiras, E.; Jarillo-Herrero, P. Unconventional Superconductivity in Magic-Angle Graphene Superlattices. *Nature* **2018**, *556*, 43–50.
- (115) Kushnir, K.; Wang, M.; Titova, L. V.; Qin, Y.; Li, G.; Tongay, S.; Koski, K. Terahertz Emission from 2D Nanomaterials. *Proc. SPIE* 10756, Terahertz Emitters, Receivers, and Applications IX 2018, 107560S.
- (116) Oh, J. Y.; Lee, J. H.; Han, S. W.; Chae, S. S.; Bae, E. J.; Kang, Y. H.; Choi, W. J.; Cho, S. Y.; Lee, J. O.; Baik, H. K.; Lee, T., Il Chemically Exfoliated Transition Metal Dichalcogenide Nanosheet-Based Wearable Thermoelectric Generators. *Energy Environ. Sci.* **2016**, 9 (5), 1696–1705.
- (117) Lee, T. Il; Jegal, J. P.; Park, J. H.; Choi, W. J.; Lee, J. O.; Kim, K. B.; Myoung, J. M. Three-Dimensional Layer-by-Layer Anode Structure Based on Co3O4 Nanoplates Strongly Tied by Capillary-like Multiwall Carbon Nanotubes for Use in High-Performance Lithium-Ion Batteries. *ACS Appl. Mater. Interfaces* **2015**, *7* (7), 3861–3865.
- (118) Yang, Y.; Li, J.; Yin, J.; Xu, S.; Mullan, C.; Taniguchi, T.; Watanabe, K.; Geim, A. K.; Novoselov, K. S.; Mishchenko, A. In Situ Manipulation of van Der Waals Heterostructures for Twistronics. *Sci. Adv.* **2020**, *6* (49), No. eabd3655.
- (119) Kose, O.; Tran, A.; Lewis, L.; Hamad, W. Y.; MacLachlan, M. J. Unwinding a Spiral of Cellulose Nanocrystals for Stimuli-Responsive Stretchable Optics. *Nat. Commun.* **2019**, *10*, 510.
- (120) Ruggiero, M. T.; Sibik, J.; Orlando, R.; Zeitler, J. A.; Korter, T. M. Measuring the Elasticity of Poly-l-Proline Helices with Terahertz Spectroscopy. *Angew. Chem., Int. Ed.* **2016**, *55* (24), *6877*–*6881*.
- (121) Salunkhe, R. R.; Kaneti, Y. V.; Yamauchi, Y. Metal-Organic Framework-Derived Nanoporous Metal Oxides toward Supercapacitor Applications: Progress and Prospects. *ACS Nano* **2017**, *11* (6), 5293–5308.
- (122) Zhu, C.; Xia, Q.; Chen, X.; Liu, Y.; Du, X.; Cui, Y. Chiral Metal-Organic Framework as a Platform for Cooperative Catalysis in Asymmetric Cyanosilylation of Aldehydes. *ACS Catal.* **2016**, *6* (11), 7590–7596.
- (123) Pan, M.; Zhao, Y.; Zeng, X.; Zou, J. Efficient Absorption of CO2 by Introduction of Intramolecular Hydrogen Bonding in Chiral Amino Acid Ionic Liquids. *Energy Fuels* **2018**, 32 (5), 6130–6135.
- (124) Herm, Z. R.; Wiers, B. M.; Mason, J. A.; van Baten, J. M.; Hudson, M. R.; Zajdel, P.; Brown, C. M.; Masciocchi, N.; Krishna, R.; Long, J. R. Separation of Hexane Isomers in a Metal-Organic Framework with Triangular Channels. *Science* **2013**, *340* (May), 960–
- (125) Lee, H. E.; Ahn, H. Y.; Mun, J.; Lee, Y. Y.; Kim, M.; Cho, N. H.; Chang, K.; Kim, W. S.; Rho, J.; Nam, K. T. Amino-Acid- A Nd Peptide-Directed Synthesis of Chiral Plasmonic Gold Nanoparticles. *Nature* **2018**, *556*, 360–364.
- (126) Xu, L.; Wang, X.; Wang, W.; Sun, M.; Choi, W. J.; Kim, J. Y.; Hao, C.; Li, S.; Qu, A.; Lu, M.; Wu, X.; Colombari, F. M.; Gomes, W. R.; Blanco, A. L.; de Moura, A. F.; Guo, X.; Kuang, H.; Kotov, N. A.; Xu, C. Enantiomer-Dependent Immunological Response to Chiral Nanoparticles. *Nature* **2022**, *601*, 366–373.
- (127) Imaz, I.; Rubio-Martínez, M.; Saletra, W. J.; Amabilino, D. B.; Maspoch, D. Amino Acid Based Metal-Organic Nanofibers. *J. Am. Chem. Soc.* **2009**, *131* (51), 18222–18223.
- (128) Zhao, J.; E, Y.; Williams, K.; Zhang, X. C.; Boyd, R. W. Spatial Sampling of Terahertz Fields with Sub-Wavelength Accuracy via Probe-Beam Encoding. *Light Sci. Appl.* **2019**, *8*, 55.
- (129) Lee, T. Il; Choi, W. J.; Moon, K. J.; Choi, J. H.; Kar, J. P.; Das, S. N.; Kim, Y. S.; Baik, H. K.; Myoung, J. M. Programmable Direct-Printing Nanowire Electronic Components. *Nano Lett.* **2010**, *10* (3), 1016–1021.

- (130) Lee, T. Il; Choi, W. J.; Kar, J. P.; Kang, Y. H.; Jeon, J. H.; Park, J. H.; Kim, Y. S.; Baik, H. K.; Myoung, J. M. Electrical Contact Tunable Direct Printing Route for a ZnO Nanowire Schottky Diode. Nano Lett. 2010, 10 (9), 3517-3523.
- (131) Choi, W. J.; Chung, Y. J.; Kim, Y. H.; Han, J.; Lee, Y. K.; Kong, K. J.; Chang, H.; Lee, Y. K.; Kim, B. G.; Lee, J. O. Drawing Circuits with Carbon Nanotubes: Scratch-Induced Graphoepitaxial Growth of Carbon Nanotubes on Amorphous Silicon Oxide Substrates. Sci. Rep. 2015, 4, 5289.
- (132) Hunsche, S.; Koch, M.; Brener, I.; Nuss, M. THz Near-Field Imaging. Opt. Commun. 1998, 150 (1-6), 22-26.
- (133) Yang, Z.; Tang, D.; Hu, J.; Tang, M.; Zhang, M.; Cui, H. L.; Wang, L.; Chang, C.; Fan, C.; Li, J.; Wang, H. Near-Field Nanoscopic Terahertz Imaging of Single Proteins. Small 2021, 17 (3), 2005814. (134) Moon, K.; Do, Y.; Park, H.; Kim, J.; Kang, H.; Lee, G.; Lim, J. H.; Kim, J. W.; Han, H. Computed Terahertz Near-Field Mapping of Molecular Resonances of Lactose Stereo-Isomer Impurities with Sub-Attomole Sensitivity. Sci. Rep. 2019, 9, 16915.
- (135) Shaban, H. A.; Valades-Cruz, C. A.; Savatier, J.; Brasselet, S. Polarized Super-Resolution Structural Imaging inside Amyloid Fibrils Using Thioflavine T. Sci. Rep. 2017, 7 (1), 12482.
- (136) Park, H.; Son, J. H. Machine Learning Techniques for THz Imaging and Time-Domain Spectroscopy. Sensors 2021, 21 (4), 1186. (137) Jiang, Y.; Li, G.; Ge, H.; Wang, F.; Li, L.; Chen, X.; Lu, M.; Zhang, Y. Machine Learning and Application in Terahertz Technology: A Review on Achievements and Future Challenges. IEEE Access 2022, 10, 53761-53776.
- (138) You, C.; Liu, J.; Wang, K.; Wang, T.; Yang, Z.; Long, Z. Terahertz Image Super-Resolution Based on a Deep Convolutional Neural Network. Appl. Opt. 2019, 58 (10), 2731-2735.
- (139) Mao, Q. I.; Zhu, Y.; Lv, C.; Lu, Y.; Yan, X.; Yan, S.; Liu, J. Convolutional Neural Network Model Based on Terahertz Imaging for Integrated Circuit Defect Detections. Opt. Express 2020, 28 (4), 5000-5012.
- (140) Cao, C.; Zhang, Z.; Zhao, X.; Zhang, T. Terahertz Spectroscopy and Machine Learning Algorithm for Non-Destructive Evaluation of Protein Conformation. Opt. Quantum Electron. 2020, 52, 225.
- (141) Liu, W.; Zhang, R.; Zhang, R.; Ling, Y.; Tang, H.; She, R.; She, R.; Wei, G.; Wei, G.; Gong, X.; Lu, Y.; Lu, Y. Automatic Recognition of Breast Invasive Ductal Carcinoma Based on Terahertz Spectroscopy with Wavelet Packet Transform and Machine Learning. Biomed. Opt. Express 2020, 11 (2), 971-981.
- (142) Liu, H.; Zhang, Z.; Zhang, X.; Yang, Y.; Zhang, Z.; Liu, X.; Wang, F.; Han, Y.; Zhang, C. Dimensionality Reduction for Identification of Hepatic Tumor Samples Based on Terahertz Time-Domain Spectroscopy. IEEE Trans. Terahertz Sci. Technol. 2018, 8 (3), $271-\overline{2}77$.
- (143) Peng, Y.; Shi, C.; Wu, X.; Zhu, Y.; Zhuang, S. Terahertz Imaging and Spectroscopy in Cancer Diagnostics: A Technical Review. BME Front. 2020, 2020, 2547609.
- (144) Guo, S.; Popp, J.; Bocklitz, T. Chemometric Analysis in Raman Spectroscopy from Experimental Design to Machine Learning-Based Modeling. Nat. Protoc. 2021, 16, 5426-5459.
- (145) Li, Q.; Fan, H.; Bai, Y.; Li, Y.; Ikram, M.; Wang, Y. K.; Huo, Y. P.; Zhang, Z. Deep Learning for Circular Dichroism of Nanohole Arrays. New J. Phys. 2022, 24, 063005.
- (146) Vermeyen, T.; Brence, J.; Van Echelpoel, R.; Aerts, R.; Acke, G.; Bultinck, P.; Herrebout, W. Exploring Machine Learning Methods for Absolute Configuration Determination with Vibrational Circular Dichroism. Phys. Chem. Chem. Phys. 2021, 23, 19781-19789.
- (147) Westermayr, J.; Gastegger, M.; Schütt, K. T.; Maurer, R. J. Perspective on Integrating Machine Learning into Computational Chemistry and Materials Science. J. Chem. Phys. 2021, 154, 230903.
- (148) Chmiela, S.; Sauceda, H. E.; Müller, K. R.; Tkatchenko, A. Towards Exact Molecular Dynamics Simulations with Machine-Learned Force Fields. Nat. Commun. 2018, 9, 3887.
- (149) Ye, S.; Zhong, K.; Zhang, J.; Hu, W.; Hirst, J. D.; Zhang, G.; Mukamel, S.; Jiang, J. A Machine Learning Protocol for Predicting

- Protein Infrared Spectra. J. Am. Chem. Soc. 2020, 142 (45), 19071-
- (150) Zhao, L.; Zhang, J.; Zhang, Y.; Ye, S.; Zhang, G.; Chen, X.; Jiang, B.; Jiang, J. Accurate Machine Learning Prediction of Protein Circular Dichroism Spectra with Embedded Density Descriptors. JACS Au 2021, 1 (12), 2377-2384.
- (151) Gastegger, M.; Behler, J.; Marquetand, P. Machine Learning Molecular Dynamics for the Simulation of Infrared Spectra. Chem. Sci. **2017**, 8 (10), 6924–6935.
- (152) Jumper, J.; Evans, R.; Pritzel, A.; Green, T.; Figurnov, M.; Ronneberger, O.; Tunyasuvunakool, K.; Bates, R.; Žídek, A.; Potapenko, A.; Bridgland, A.; Meyer, C.; Kohl, S. A. A.; Ballard, A. J.; Cowie, A.; Romera-Paredes, B.; Nikolov, S.; Jain, R.; Adler, J.; Back, T.; Petersen, S.; Reiman, D.; Clancy, E.; Zielinski, M.; Steinegger, M.; Pacholska, M.; Berghammer, T.; Bodenstein, S.; Silver, D.; Vinyals, O.; Senior, A. W.; Kavukcuoglu, K.; Kohli, P.; Hassabis, D. Highly Accurate Protein Structure Prediction with AlphaFold. Nature 2021, 596, 583-589.
- (153) Tunyasuvunakool, K.; Adler, J.; Wu, Z.; Green, T.; Zielinski, M.; Žídek, A.; Bridgland, A.; Cowie, A.; Meyer, C.; Laydon, A.; Velankar, S.; Kleywegt, G. J.; Bateman, A.; Evans, R.; Pritzel, A.; Figurnov, M.; Ronneberger, O.; Bates, R.; Kohl, S. A. A.; Potapenko, A.; Ballard, A. J.; Romera-Paredes, B.; Nikolov, S.; Jain, R.; Clancy, E.; Reiman, D.; Petersen, S.; Senior, A. W.; Kavukcuoglu, K.; Birney, E.; Kohli, P.; Jumper, J.; Hassabis, D. Highly Accurate Protein Structure Prediction for the Human Proteome. Nature 2021, 596, 590-596.
- (154) Long, G.; Sabatini, R.; Saidaminov, M. I.; Lakhwani, G.; Rasmita, A.; Liu, X.; Sargent, E. H.; Gao, W. Chiral-Perovskite Optoelectronics. Nat. Rev. Mater. 2020, 5, 423-439.
- (155) Yang, S. H.; Naaman, R.; Paltiel, Y.; Parkin, S. S. P. Chiral Spintronics. Nat. Rev. Phys. 2021, 3, 328-343.
- (156) Zhang, Y.; Guo, J.; Shi, L.; Zhu, Y.; Hou, K.; Zheng, Y.; Tang, Z. Tunable Chiral Metal Organic Frameworks toward Visible Light-Driven Asymmetric Catalysis. Sci. Adv. 2017, 3 (8), No. e1701162.

□ Recommended by ACS

Enhanced Chemical Sensing with Multiorder Coherent Raman Scattering Spectroscopic Dephasing

Hanlin Zhu, Delong Zhang, et al.

MAY 27, 2022

ANALYTICAL CHEMISTRY

READ 2

Ultrashort Pulse Excited Tip-Enhanced Raman Spectroscopy in Molecules

Yang Luo, Klaus Kern, et al.

JUNE 15, 2022 NANO LETTERS

READ

Molecular Optomechanics Approach to Surface-Enhanced **Raman Scattering**

Ruben Esteban, Javier Aizpurua, et al.

JULY 01, 2022

ACCOUNTS OF CHEMICAL RESEARCH

READ **C**

Alkyne-Tagged Raman Probes for Local Environmental Sensing by Hydrogen-Deuterium Exchange

Xiaotian Bi, Lu Wei, et al.

MAY 04, 2022

JOURNAL OF THE AMERICAN CHEMICAL SOCIETY

READ 2

Get More Suggestions >